Research article

Ketogenic diet enhances cognitive-behavioral function and hippocampal neurogenesis while attenuating amyloid pathology in Tg-SwDI mice

Journal of Alzheimer's Disease
1–24

DOI: 10.1177/13872877261445916
journals.sagepub.com/home/alz

Victoria E. Pulido-Correa[1], Ariana V. Hernandez[1], Eleanor J. Wind[1], YingYing Zhu[1], Chana Vogel[1], Shaina Binu[1], Mikayla Jeneske[1], Dylan Kuni[1], Vedika Chiduruppa[1], Bianca Echeverria[1], Lauren Rosenberg[1] and Lisa S. Robison[1]

Abstract

Background: The ketogenic diet (KD), characterized by high-fat, low-carbohydrate, and moderate protein intake, has gained attention for its therapeutic potential in patients with neurodegenerative diseases, including Alzheimer's disease (AD). Studies in AD rodent models report that KD and/or ketogenic supplements attenuate cognitive-behavioral impairments, neuroinflammation, amyloid-β (Aβ) plaques, and tau pathology. However, it is unknown whether KD can similarly benefit individuals with cerebral amyloid angiopathy (CAA), a prevalent condition in which Aβ accumulates in cerebral vessels. CAA is highly comorbid with AD and, on its own, increases the risk of stroke, cognitive impairment, and dementia, yet no effective treatments currently exist.

Objective: To determine whether KD can improve cognitive-behavioral and neuropathological outcomes in a mouse model with CAA.

Methods: Male Tg-SwDI mice were fed either a standard chow or KD from 3.5 to 7.5 months of age. Following ~3 months of dietary intervention, glucose and ketone body levels were assessed, then mice underwent a battery of behavioral tests to evaluate locomotor activity, anxiety-related behaviors, and cognition. Immunohistochemistry was performed to assess amyloid pathology, vascular density, neuroinflammation, white matter integrity, and hippocampal neurogenesis.

Results: In addition to KD inducing nutritional ketosis and achieving metabolic benefits, mice on KD exhibited increased activity, enhanced spatial learning and memory, and a trend toward improved spatial working memory. These cognitive benefits were accompanied by an attenuation of amyloid pathology and increased hippocampal neurogenesis.

Conclusions: These findings suggest that a KD may be safe and effective in AD and dementia patients with CAA.

Keywords

Alzheimer's disease, amyloid, cerebral amyloid angiopathy, cerebrovascular disorders, dementia, ketogenic diet, neurogenesis

Received: 25 February 2025; accepted: 4 March 2026

Introduction

Cerebral amyloid angiopathy (CAA), the accumulation of amyloid peptides (most commonly amyloid-β; Aβ) in the cerebral vasculature, is one of the most prevalent forms of cerebral small vessel disease. Most CAA cases are sporadic and associated with aging, though familial forms exist. As a single pathology, CAA can result in vascular cognitive impairment and dementia and significantly increases the risk of stroke.[1,2] One of the most significant clinical consequences of CAA is the increased risk of intracerebral hemorrhages. These can be large or small (microbleeds), and recurrent hemorrhages are common. Although hemorrhages are more common, CAA can also lead to ischemic events, including transient ischemic attacks and strokes. The progressive accumulation of amyloid in

[1]Department of Psychology and Neuroscience, Nova Southeastern University, Fort Lauderdale, FL, USA

Corresponding author:
Lisa S. Robison, Department of Psychology and Neuroscience, Nova Southeastern University, 3300 S. University Drive, Fort Lauderdale, FL, USA.
Email: lrobiso1@nova.edu

Handling Associate Editor: Melissa Barker-Haliski

vessel walls can narrow the lumen of the vessels, leading to chronic hypoperfusion. This reduced blood flow can cause gradual damage to brain tissue, contributing to cognitive decline. Indeed, CAA is specifically linked to impairments in several cognitive domains, including perceptual speed and episodic memory.[1] CAA can also be associated with inflammation characterized by activated microglia and reactive astrocytes that produce pro-inflammatory cytokines and chemokines, reactive oxygen and nitrogen species, and activation of the complement pathway.[2] Of note, CAA is commonly found in patients with Alzheimer's disease (AD)[3]; this overlap can exacerbate cognitive decline and other neurological symptoms.[4] The high rate of comorbidity is perhaps unsurprising, as both CAA and AD are characterized by the accumulation of Aβ, albeit differing in their distribution (blood vessel walls in CAA versus brain parenchyma in AD). The processes that govern Aβ clearance and deposition are common to both diseases. Indeed, CAA likely contributes to AD pathology by impairing perivascular Aβ drainage from the brain, a major route of Aβ clearance.[5,6]

Currently, there is no cure for CAA, nor are there any FDA-approved treatments. Recently approved Aβ-directed monoclonal antibodies (e.g., lecanemab) facilitate parenchymal Aβ removal in patients with AD; however, these treatments have questionable benefits for cognition and carry substantial risk for amyloid-related imaging abnormalities (ARIA), including brain swelling (edema) and bleeding (hemorrhage).[7,8–10] ARIA resulting from the treatment of AD with Aβ-directed monoclonal antibodies may be of particular concern in individuals with CAA.[8–11] In fact, it was recently hypothesized that patients who are positive for CAA should be identified and excluded from anti-amyloid therapy.[12] Therefore, novel interventions are necessary for patients with CAA when present either as a singular pathology or in cases where CAA is comorbid with AD.

One potential nonpharmacological intervention for CAA that has yet to be tested is the ketogenic diet, which involves the consumption of limited carbohydrates (usually <5%), moderate protein intake, and very high levels of fat.[13] Limiting the intake of carbohydrates induces a state of "nutritional ketosis" that promotes ketogenesis while reducing gluconeogenesis.[13] This causes ketone bodies to replace glucose as the body's primary energy source. Originally used for the treatment of epilepsy, the ketogenic diet has gained considerable attention in recent decades for its ability to produce quick weight loss and improve metabolic outcomes, such as those related to prediabetes/Type II diabetes (e.g., insulin resistance, blood glucose).[14,15] Additionally, growing evidence supports the efficacy of the ketogenic diet in promoting brain health and improving cognitive performance across a number of domains, including working memory, reference memory, and attention.[16] Notably, the ketogenic diet has been found to be protective in a variety of neurodegenerative diseases, including AD, Parkinson's disease, and motor neuron disease.[17] Emerging research suggests that consumption of a ketogenic diet or supplementation with exogenous ketones exerts many beneficial effects, including cognitive-boosting, pro-neurogenic, anti-inflammatory, and antioxidant effects.[18–21] Studies in AD rodent models have found that ketogenic diet and/or exogenous treatment with ketone supplements attenuate cognitive-behavioral impairments, neuroinflammation, oxidative stress, and Aβ accumulation; and enhance mitochondrial function and synaptic plasticity.[20] A review of the use of either ketogenic diet or exogenous ketone supplementation reported that these ketogenic dietary interventions provide treatment benefits in AD patients; however, most studies are small, uncontrolled, and involve relatively short treatment periods.[22]

There is evidence to suggest that ketogenic dietary interventions promote brain health and enhance cognitive performance, are protective against neurodegenerative diseases, including AD, and aid in the recovery from cerebrovascular events, such as stroke.[16,18,20,22,23] However, it has yet to be determined whether the ketogenic diet can similarly benefit patients with CAA. Here, we used a transgenic mouse model with CAA (Tg-SwDI mice) to test the hypothesis that chronic consumption of a ketogenic diet during early-to-moderate disease stages will improve cognitive-behavioral and neuropathological outcomes.

Methods

Animals and housing conditions

All experiments were approved by the Institutional Animal Care and Use Committee at Nova Southeastern University (Davie, FL, USA), and compliance was maintained with the ARRIVE guidelines.[24] Male Tg-SwDI mice (JAX MMRRC stock #034843) were bred for this experiment at Nova Southeastern University using mice purchased from Jackson Laboratory (Bar Harbor, ME). These mice carry three mutations in the human amyloid-β protein precursor (AβPP) gene: Iowa (APP/D694N), Dutch (APP/E693Q), and Swedish (K670N/M671L). These mutations lead to the accumulation of fibrillar Aβ peptides in the cerebral vasculature, effectively replicating the key pathological features of CAA.[25] Tg-SwDI mice also exhibit cerebrovascular dysfunction, neuroinflammation, and cognitive-behavioral impairment, as we and others have previously shown.[25–29] Animals were housed in groups of three to four in standard polysulfone cages (dimensions: 7.75""L × 14.75""W × 5.25""H). The housing facility was kept on a reversed 12-h light-dark cycle (lights on at 8:00 PM and off at 8:00 AM) to mimic the natural circadian rhythm of the mice. Temperature and humidity were set at 68–72°&degF and 40–60%, respectively. These conditions were monitored and recorded daily to ensure a stable and comfortable environment conducive to the mice's

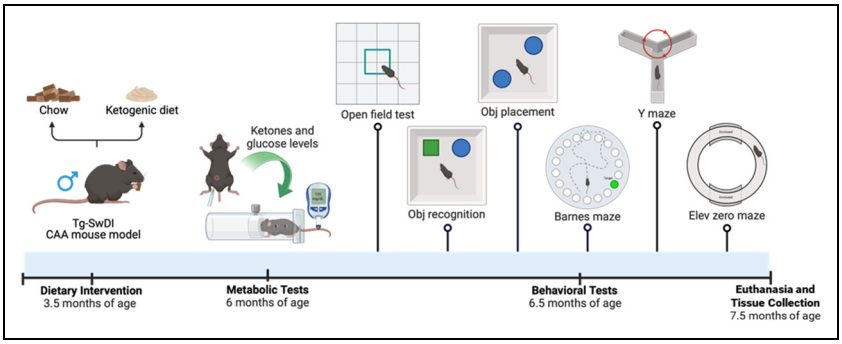

Figure 1. Timeline of the experiment. Male Tg-SwDI mice either remained on standard rodent chow or were switched to a ketogenic diet at ~3.5 months of age, and the assigned diet was maintained for the duration of the study. At 6 months of age, metabolic testing was performed to assess blood ketone body and glucose levels in the fed and fasting states, as well as glucose tolerance. Behavior testing was then performed to assess locomotor activity, anxiety-like behavior, and cognition, followed by euthanasia and tissue collection at ~7.5 months of age.

physiological needs. Mice were given ad libitum access to fresh food and water and were provided with various environmental enrichment items (plastic huts, chew bones, nesting materials) for the duration of the study. All work with mice was performed during the dark cycle.

Diet intervention

A timeline of the experiment is shown in Figure 1. All mice were fed a standard chow diet until approximately 3.5 months of age. At that point, mice were either switched to a ketogenic diet (n = 8) or maintained on the standard chow diet (n = 7) for the duration of the study (~4 months). The Ketogenic Diet AIN-76A Modified (Catalog #F3666, Bio-Serv, Flemington, NJ) was composed of 93.4% fat, 4.7% protein, and 1.8% carbohydrates, and had a caloric value of 7.24 kcal/g. The ingredients of the ketogenic diet included lard, butter, corn oil, casein, cellulose, mineral mix, vitamin mix, and dextrose. The standard chow diet (5P76, LabDiet, St. Louis, MO) was composed of 14.4% fat, 26.1% protein, and 59.5% carbohydrates. Mice were weighed and food was replenished twice weekly. Average food and fluid intake per mouse were calculated for each cage based on the total amount consumed divided by the number of mice housed in the cage; food (kcal) and fluid (mL) consumption were then normalized to body weight.

Ketone body levels, blood glucose levels, and glucose tolerance testing

Ketone body levels, fasting blood glucose levels, fed blood glucose levels, and glucose tolerance were assessed at approximately 6 months of age. Ketone body levels and fed blood glucose levels were measured in the fed state ~2–4 h into the dark cycle using a Precision Xtra blood ketone meter and a Prodigy Autocode glucometer, respectively. Blood (~3–5 µL) was collected via tail snip (<1 mm) following application of topical analgesic (Aspercreme).

Mice underwent a glucose tolerance test on a subsequent day to assess diabetic status. Mice were fasted for ~16 h, and their fasting blood glucose levels were measured (t = 0) using a Prodigy Autocode glucometer with blood collected via tail snip (<1 mm) following application of topical analgesic (Aspercreme). Following an intraperitoneal injection of 2 g/kg of glucose, blood glucose levels were measured at 15, 30, 60, 90, and 120 min post-injection to assess glucose tolerance. Approximately 3–5 µL of blood was collected at each time point.

Behavior testing

Three months after diet initiation, mice were subjected to a battery of behavioral tests, including the open field test, novel object recognition test, object placement test, Y-maze, elevated zero maze, and Barnes maze. Mice were acclimated to the behavior testing room for at least 30 min prior to the start of testing. Following each trial, behavioral equipment and any objects used during testing were cleaned with 70% isopropyl alcohol and allowed to dry thoroughly before the next animal was assessed.

Open field. An open field test was performed to assess general activity levels/exploratory behavior and anxiety-like behavior. Mice were placed into an open field arena (46 cm×46 cm×46 cm; opaque white acrylic walls and floor), and behavior was recorded for 10 min. Distance traveled, time spent moving, speed, and center activity were quantified using automated software (Noldus EthoVision v17, Wageningen, the Netherlands), while measures of rearing and grooming behavior were manually recorded by two independent raters blinded to the experimental condition.

Novel object recognition test (NORT). NORT was performed to assess object recognition memory using two trials, both of which were performed in the open field arena. In the first trial (training), mice were placed in the arena with two identical objects and allowed to explore for 10 min. Mice were then returned to their home cage for a 1-h retention period, after which mice were placed back into the arena for the second trial (test). In the test trial, there were two objects in the arena in the same location as during training: one "familiar" object (previously exposed to during the training trial) and one "novel" object. The time spent exploring each object was recorded for 5 min and measured using automated software (Noldus EthoVision v17, Wageningen, the Netherlands), with intact memory determined by more interaction with the novel object versus the familiar object. The discrimination index was calculated as [(time with novel object – time with familiar object)/time with both objects].

Object placement test (OPT). OPT was performed to assess spatial memory using two trials, both of which were performed in the open field arena. In the first trial (training), mice were placed in the arena with two identical objects and allowed to explore for 10 min. Mice were then returned to their home cage for a 1-h retention period, after which mice were placed back into the arena for the second trial (test). In the test trial, the same two objects were placed in the arena as in the training trial. This included one object in a "familiar" location (same as in the training trial) and one "displaced" object (location switched from the previous training trial). The time spent exploring each object was recorded for 5 min and measured using automated software (Noldus EthoVision v17, Wageningen, the Netherlands), with intact memory determined by more interaction with the displaced object versus the familiar object. The discrimination index was calculated as [(time with displaced object – time with familiar object)/time with both objects].

Y-maze. The Y-maze was performed to assess spatial working memory. Each mouse received one 5-min trial performed in a Y-shaped maze consisting of three opaque arms positioned at a 120° angle from each other (each arm = 30 cm L × 6 cm W × 15 cm H). The order of arm entries was recorded by an experimenter blinded to the experimental conditions, and the total number of arm entries was counted as a measure of exploratory behavior. Rodents typically prefer to explore a new arm of the maze instead of returning to one that they have previously visited.[30] Over the course of multiple arm entries, subjects should alternate the arms visited, showing a tendency to enter a less recently visited arm. The number of triads (a sequence of each of the three arms visited) was recorded in order to calculate the percentage of alternation. An entry into an arm was only counted when all four paws were within that arm. Spontaneous alternation (indicative of intact spatial working memory) was calculated as ([# triads/(total # arm entries – 2)] × 100). Additional outcome measures assessed for the Y-maze include same arm return, alternate arm return, arm preference, distance traveled, and velocity (speed while moving).

Elevated zero maze. The elevated zero maze was performed to assess anxiety-like behavior. The elevated zero maze is composed of a circular "O"-shaped platform divided into 2 closed sections (high walls surrounding the edges) and 2 open sections (no surrounding walls). Each mouse underwent a single 5-min trial that began by placing the mouse into a closed portion of the maze. The number of entries into the open areas and the time spent in or near the open sections were recorded as measures of reduced anxiety-like behavior measured using automated software (Noldus EthoVision v17, Wageningen, the Netherlands).

Barnes maze. The Barnes maze was performed to assess spatial learning and memory. The maze consists of an elevated circular white platform (diameter = 122 cm) with 40 evenly spaced holes around the perimeter. One hole was deemed the "target hole," which had a cup mounted underneath it, while the remaining 39 holes were left empty. Because bright light and open spaces are aversive, mice are motivated to locate and enter the cup beneath the escape hole. The location of the target hole was kept constant throughout the habituation and training trials.

Day 1 consisted of a single habituation trial. During habituation, mice were placed in the escape cup for 1 min and covered with a clear glass beaker. Mice were then placed in the center of the arena and covered with an opaque beaker for 15 s prior to the start of the 5-min exploration period. The exploration period lasted 5 min, regardless of whether the mouse entered the escape cup. At the end of the 5 min, mice were placed in the escape cup and covered with a clear glass beaker for 1 min, after which they were returned to their home cage.

Days 2–4 consisted of 2 training trials per day, with trials separated by approximately 1 h. At the start of each trial, mice were placed in the center of the arena and covered with an opaque beaker for 15 s prior to the start of each training trial. Mice were then given a maximum of 3 min to find and enter the escape cup, at which point the trial ended, and they were covered with a clear glass beaker for 1 min. If a mouse did not enter the escape cup within 3 min, it was gently guided to the escape cup and covered with a clear glass beaker for 1 min before being returned to its home cage. The latency to find the escape cup across the 6 total training trials was calculated as a measure of spatial learning using automated software (Noldus EthoVision v17, Wageningen, the Netherlands). Additional measures assessed for Barnes maze training

trials include path efficiency, success rate for finding the target hole, total errors (entries to non-target holes), reference memory errors (initial entry into a non-target hole during a trial), and working memory errors (repeated entries into the same non-target hole within a single trial). For trials in which a mouse did not find the target hole, a score of "0" was assigned for path efficiency, while for all error types, a value of the maximum score +1 was assigned.

On day 5, a single probe trial was conducted ~24 h after the last training trial (1-day probe). Mice were placed in the center of the arena and covered with an opaque beaker for 15 s prior to the start of the trial. The escape cup was removed from the arena for the probe trials. The exploration period lasted 2 min for each mouse. An additional probe trial was conducted 7 days after the last training trial to assess longer-term spatial memory (7-day probe). For each trial, automated tracking software (Noldus EthoVision v17, Wageningen, the Netherlands) was used to determine the primary latency (latency to first target hole visit) and the time spent in the target quadrant where the escape cup had previously been located. Additional measures assessed for Barnes maze training trials include path efficiency, success rate for finding the target hole, and velocity (speed of travel while mouse was active).

Euthanasia and tissue collection

Euthanasia and tissue collection were performed after completion of all behavior testing. Mice were deeply anesthetized with isoflurane anesthesia (5% induction; ~3–4% maintenance), underwent transcardial perfusion with ice-cold 0.9% NaCl, and were decapitated to allow for brain extraction. Adipose tissue (visceral and subcutaneous fat) was dissected and weighed. Brains were collected and bisected; one hemisphere was fixed, and the other was flash-frozen. The fixed hemisphere was immersed in 4% paraformaldehyde (PFA) for 48 h and then cryopreserved in 30% sucrose containing 0.01% sodium azide, both at 4 °C. The flash-frozen hemisphere was frozen in 2-methylbutane over dry ice, then stored at −80 °C until use.

Immunofluorescence

Fixed brain hemispheres were embedded in OCT and cut on a cryostat at ~18 °C into 4 sets of 40 μM sagittal free-floating sections. Free-floating immunohistochemistry was performed to assess glial markers [ionized calcium-binding adapter molecule 1 (Iba1; microglia) and glial fibrillary acidic protein (GFAP; astrocytes)], as well as white matter integrity (myelin basic protein; MBP) and neurogenesis markers [doublecortin (DCX), a measure of neuroblasts/immature neurons, and Ki-67, a marker of cell proliferation).

Sections were washed in 1x PBS containing 0.01% sodium azide (3 × 3 min at room temperature), permeabilized in 0.3% Triton X-100 in 1x PBS with 0.01% sodium azide (30 min at room temperature), and blocked in 4% donkey serum with 0.3% Triton X-100 in 1x PBS with 0.01% sodium azide (30 min at room temperature). Sections were then incubated with primary antibodies overnight at 4 °C. Primary antibodies were diluted in blocking buffer and included: rabbit anti-Iba1 (1:1000; Cat #019-19741, Fujifilm Wako, Richmond, VA), rabbit anti-GFAP (1:100; Cat #PB9082, Boster Bio, Pleasanton, CA), guinea pig anti-DCX (1:1000; Cat #AB2253, Millipore, Burlington, MA), rabbit anti-MBP (1:200; Cat #10458-1-AP, Proteintech, Rosemont, IL), and rat anti-Ki67 (1:200; Cat #14-5698-82, Invitrogen, Waltham, MA). The following day, sections were washed with 1x PBS with 0.01% sodium azide (3 × 3 min at room temperature) and incubated for 1 h at room temperature with secondary antibodies diluted in blocking buffer. Secondary antibodies included: donkey anti-guinea pig 488 (1:300; Cat #706-545-148, Jackson Immunoresearch, West Grove, PA), donkey anti-rabbit 594 (1:300; Cat #A21206, Invitrogen, Waltham, MA), donkey anti-rabbit 594 (1:300; Cat #711-585-152, Jackson Immunoresearch, West Grove, PA), and donkey anti-rat 647 (1:300; Cat #A78947, Invitrogen, Waltham, MA). Sections were then washed with 1x PBS with 0.01% sodium azide (3 × 3 min at room temperature) prior to being mounted onto glass microscope slides using Prolong Gold Antifade mounting media with DAPI counterstain.

Fresh frozen brain hemispheres were cut on a cryostat at ~13 °C into 3 sets of 20 μM sagittal sections, thaw-mounted onto charged glass microscope slides, and stored at −80 °C until use. Sections were thawed to room temperature, fixed with 4% paraformaldehyde in PBS (10 min at room temperature), washed in 1x PBS with 0.01% sodium azide (3 × 3 min at room temperature), permeabilized in 0.1% Triton X-100 in 1x PBS with 0.01% sodium azide (30 min at room temperature), and blocked in 4% donkey serum with 0.1% Triton X-100 in 1x PBS with 0.01% sodium azide (30 min at room temperature). Sections were then incubated with primary antibody overnight at 4 °C. The primary antibody solution consisted of rabbit anti-collagen IV (1:200; Cat #PA1-28534, Invitrogen, Carlsbad, California) diluted in blocking buffer. The following day, sections were washed (3 × 3 min at room temperature), then incubated for 1 h with secondary antibody solution at room temperature. The secondary antibody solution consisted of donkey anti-rabbit 594 (1:300, Cat #A21206, Invitrogen, Carlsbad, California) diluted in blocking buffer. After three additional washes (3 × 3 min at room temperature), sections were stained with 0.0125% Thioflavin-S in 50% PBS/50% EtOH (15 min at room temperature). Sections were washed with 50% PBS/50% EtOH (2 × 3 min at room temperature) then 1x PBS with 0.01%

sodium azide (3 × 3 min at room temperature) prior to being mounted with Prolong Gold Antifade mounting media.

Images were taken using a 5x or 10x objective with cellSens Imaging Software on an Olympus IX73 fluorescence microscope, or with a 20x objective using BZ-X800 Viewer Software on a Keyence BZ-X810 fluorescence microscope. For analysis of Thioflavin-S staining (amyloid), collagen IV (blood vessels), Iba1 (microglia), and GFAP (astrocytes), images were taken in the hippocampus (subiculum, dentate gyrus, CA1, and CA3), thalamus, and cortex. For analysis of MBP (myelin), images were taken in the hippocampus, corpus callosum, and cortex. For analysis of Ki67 (cell proliferation) and DCX (neurogenesis), images were taken in the dentate gyrus of the hippocampus. Representative images with annotated regions of interest are shown in Supplemental Figure 1. NIH ImageJ software was used to identify regions of interest, threshold images, and extract measures of intensity and/or % area covered for Thioflavin-S, Collagen IV, Iba-1, GFAP, and MBP in each brain region. Colocalization analysis of Thioflavin-S/Collagen IV was performed to distinguish vascular (CAA-associated) from non-vascular (parenchymal/plaque) amyloid accumulation. Plaque # was manually counted in cortical sections stained with Thioflavin-S. DCX + cells (neuroblasts/immature neurons) and Ki67 + cells (proliferating cells) were manually counted in the dentate gyrus of the hippocampus as a measure of neurogenesis. DCX + and Ki67 + cells counts were performed by two independent raters who were blinded to the experimental condition of each mouse.

Statistical analyses

Statistical analyses were performed using Prism v10.1.1 (GraphPad Software, San Diego, CA, USA). The Grubbs' test, a widely accepted method for detecting outliers in small datasets, was conducted to identify statistically significant outliers ($\alpha = 0.05$); outliers were replaced with the next most extreme value. Unpaired two-sample t-tests were conducted for data that did not include repeated measures. Two-way mixed ANOVAs followed by Holm-Sidak post hoc tests were performed for data that were collected and reported at multiple timepoints (body weight, fasting and fed blood ketone body levels, fasting and fed blood glucose levels, glucose tolerance test). One-sample t-tests were used for analysis of NOR and OPT performance (discrimination index versus hypothetical value of 0). The threshold for statistical significance was set at $p < 0.05$.

Results

Metabolic outcomes

Caloric intake. Caloric intake for each cage was approximated based on food weights and the energy density of the respective diet; these values were then normalized using the average body weight of the mice in each cage to calculate food intake in kcal/g of body weight (Figure 2(a)). An unpaired two-sample t-test showed no significant difference in caloric intake between groups [$t(3) = 0.092$, $p = 0.932$]. To ensure that palatability was acceptable to mice, consumption was assessed twice weekly during the first four weeks of ketogenic diet and compared to baseline caloric consumption (10 days of chow consumption just prior to the switch to ketogenic diet). Caloric consumption did not differ between baseline (chow) and any timepoint during ketogenic diet consumption (Supplemental Figure 2), suggesting that the diet was indeed palatable and well tolerated by the mice.

Fluid intake. Fluid intake for each cage was approximated based on water bottle weights; these values were then normalized by the average body weight of the mice in that cage to calculate fluid intake in mL/g of body weight (Figure 2(b)). An unpaired two-sample t-test showed no significant difference between treatment groups [$t(3) = 1.978$, $p = 0.142$].

Body weight. Body weight change is presented as % change from baseline (prior to diet initiation) and plotted biweekly through the duration of the experiment (Figure 2(c)). A two-way mixed ANOVA found significant main effects of diet [$F(1,104) = 80.79$, $p < 0.001$; keto < chow] and time [$F(8,104) = 29.34$, $p < 0.001$; increased weight gain over time], as well as a diet×time interaction [$F(8,104) = 37.88$, $p < 0.001$]. Multiple pairwise comparisons (Holm-Sidak) revealed that chow-fed mice displayed significant weight gain from baseline in weeks 4 through 16 ($p < 0.0001$ for all), while keto-fed mice displayed significant weight loss from baseline in weeks 2 through 16 ($p < 0.001$).

Adiposity. Adiposity was assessed by measuring the mass of subcutaneous (Figure 2(d)) and visceral (Figure 2(e)) fat pads. An unpaired two-sample t-test found no significant difference in subcutaneous fat between groups [$t(13) = 1.081$, $p = 0.150$]. However, mice fed a ketogenic diet had significantly less visceral fat compared to chow-fed mice [$t(13) = 1.810$, $p = 0.047$].

Blood ketone body levels. Blood ketone body levels were measured in both the fasting and fed state to assess nutritional ketosis (Figure 2(f)). One outlier was identified in the chow group for the measure of fed ketone body levels. A two-way mixed ANOVA found significant main effects of diet [$F(1,13) = 47.88$, $p < 0.0001$] and feeding state [$F(1,13) = 44.49$, $p < 0.0001$], as well as a diet×feeding state interaction [$F(1,13) = 6.648$, $p = 0.023$]. Multiple pairwise comparisons (Holm-Sidak) found that ketone body levels were higher in the fasted versus the fed

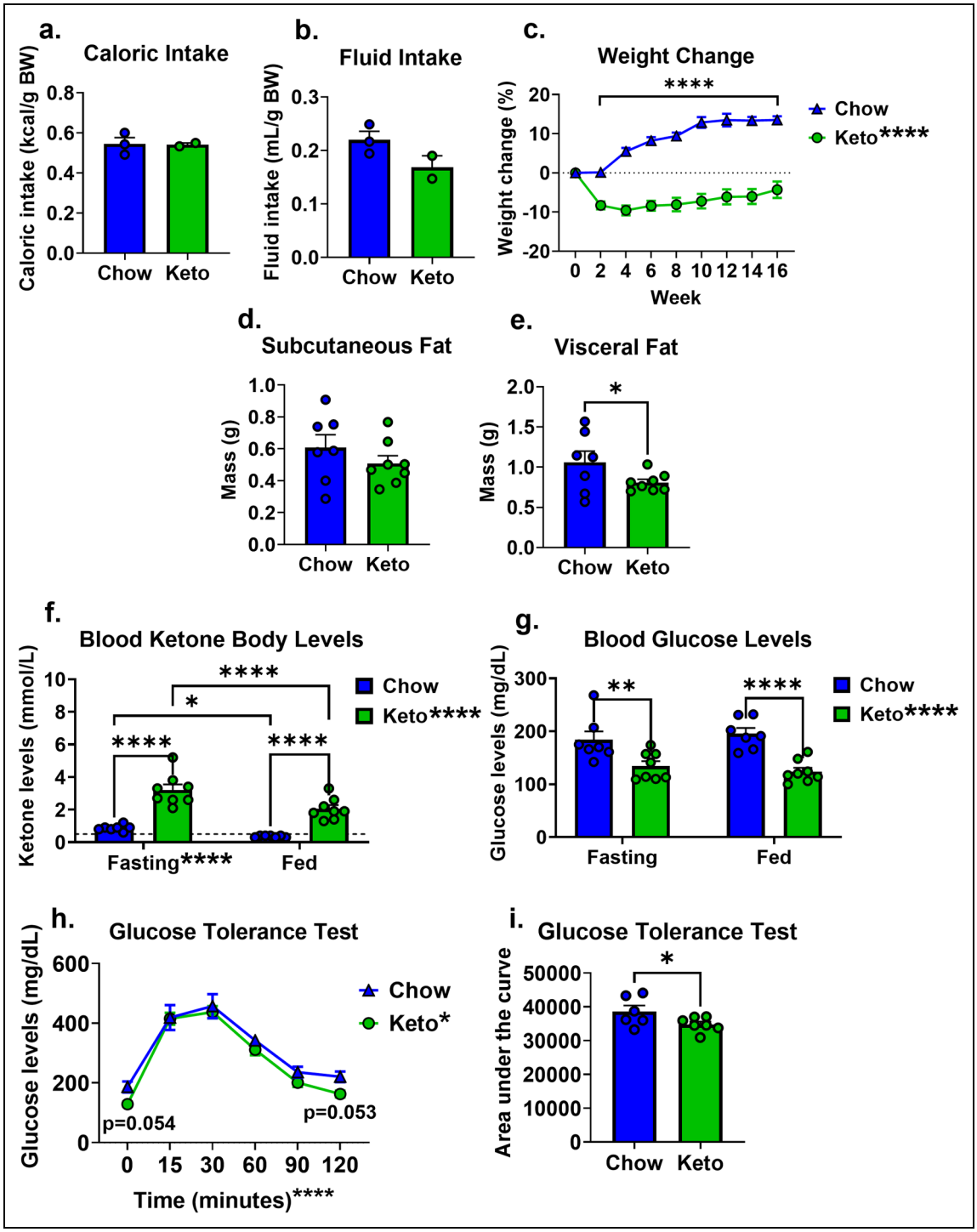

Figure 2. Ketogenic diet induced nutritional ketosis and had metabolic benefits in male Tg-SwDI mice. Caloric intake (a) and fluid intake (b) were measured biweekly, with data presented as an average value for each cage over the course of the diet intervention period. (c) Changes in body weight from baseline were measured throughout the diet intervention period. (d) Subcutaneous and (e) visceral fat were dissected and weighed at the time of euthanasia. (f) Ketone body and (g) glucose levels were measured in tail vein blood samples in both fasted and fed states. (h) Glucose tolerance test (GTT) was performed, with blood glucose levels measured at baseline in the fasted state (t = 0), and at 15, 30, 60, 90, and 120 min after a glucose challenge injection. One mouse was excluded from each group, leaving sample sizes of n = 6 for chow and n = 7 for keto. (i) Area under the curve (AUC) was calculated for data collected during the glucose tolerance test as a measure of cumulative glucose exposure. Data are presented as mean + SEM in all graphs. All statistical analyses were performed using an unpaired two-sample t-test except for the GTT data over time (h), which was analyzed using a two-way repeated measures ANOVA followed by Holm-Sidak post hoc test. *$p < 0.05$, **$p < 0.01$, ***$p < 0.001$, ****$p < 0.0001$.

condition for both chow ($p = 0.015$) and keto ($p < 0.0001$) mice, and that ketone body levels were higher in mice fed a ketogenic diet compared to mice fed a standard chow diet in both the fasting and fed conditions ($p < 0.0001$ for both).

Blood glucose levels. Blood glucose levels were measured in both the fasting and fed state (Figure 2(g)). A two-way mixed ANOVA found significant main effects of diet [$F(1,13) = 35.44$, $p < 0.0001$; keto < chow], while the main effect of feeding state [$F(1,13) = 0.0012$, $p = 0.972$] and the diet×feeding state interaction [$F(1,13) = 0.9059$, $p = 0.359$]. Multiple pairwise comparisons (Holm-Sidak) found that blood glucose levels were lower in mice fed a ketogenic diet compared to mice fed a standard chow diet in both the fasting ($p = 0.003$) and fed ($p < 0.0001$) conditions.

Glucose tolerance test. A glucose tolerance test was performed to assess diabetic status. Following measurement of fasting glucose levels, mice were injected with a bolus of glucose, with blood glucose levels measured at $t = 15$, 30, 60, 90, and 120 min post-injection (Figure 2(h)). One mouse was excluded from the chow group due to poor injection, and one outlier was identified in the ketogenic diet group. A two-way mixed ANOVA found significant main effects of diet [$F(1,12) = 5.467$, $p = 0.038$; keto < chow] and time [$F(5,60) = 77.77$, $p < 0.0001$; expected rise and fall of glucose following challenge injection], while the diet×time interaction was not significant [$F(5,60) = 0.6205$, $p = 0.685$]. Multiple pairwise comparisons (Holm-Sidak) revealed trends of attenuated blood glucose levels in mice fed a ketogenic diet compared to mice fed a standard chow diet at $t = 0$ min ($p = 0.054$) and $t = 120$ min ($p = 0.053$).

Additionally, area under the curve was calculated as a measure of cumulative glucose exposure during the glucose tolerance test (Figure 2(i)). An unpaired two-sample t-test found that mice fed a ketogenic diet displayed significantly lower AUC values compared to chow-fed mice [$t(12) = 2.007$, $p = 0.034$].

Behavior testing

Supplemental Table 1 includes effect sizes and achieved statistical power for all behavioral test outcomes.

Open field. The open field test was performed to assess general locomotor/exploratory behavior, as well as anxiety-like behavior (Figure 3(a)-(f)). Unpaired two-sample t-tests performed separately for each outcome measure found that mice fed a ketogenic diet displayed significantly greater distance traveled [$t(13) = 2.819$, $p = 0.007$, Figure 3(a)], time spent moving [$t(13) = 2.578$ $p = 0.012$, Figure 3(b)], and velocity while moving [$t(13) = 2.352$, $p = 0.018$, Figure 3(c)], while there were no group differences in time spent in the center of the arena [$t(13) = 0.4082$, $p = 0.345$, Figure 3(d)], time spent rearing [$t(13) = 0.8735$, $p = 0.199$, Figure 3(e)], nor time spent grooming [$t(13) = 0.8754$, $p = 0.199$, Figure 3(f)]. Individual track plots and heat maps for the open field are shown in Supplemental Figure 3.

Elevated zero maze. The elevated zero maze test was performed to assess anxiety-like behavior (Figure 3(g)-(i)). Unpaired two-sample t-tests performed separately for each outcome measure revealed a trend that mice fed a ketogenic diet made more entries to the open areas compared to mice fed a standard chow diet [$t(13) = 1.395$, $p = 0.093$, Figure 3(g)]; however, there were no group differences in time spent in the open areas [$t(13) = 0.1383$, $p = 0.446$, Figure 3(h)]. Additionally, time spent in the border zones of the closed areas closest to the open areas was assessed, with an unpaired two-sample t-test revealing that mice fed a ketogenic diet spent more time in these border zones compared to mice on a standard chow diet [$t(13) = 3.185$, $p = 0.004$, Figure 3(i)]. A heat map of activity in the elevated zero maze for the mean of each treatment group is shown in Figure 3(j).

Novel object recognition test (NORT). The novel object recognition test was performed to assess object recognition memory. There was no effect of diet on total time spent exploring both objects (data not shown). Performance was quantified by the discrimination index (Figure 4(a)). One outlier was identified in the ketogenic diet-fed group. One sample t-tests found that both chow-fed mice [$t(6) = 5.969$, $p = 0.001$] and keto-fed mice [$t(7) = 7.211$, $p < 0.001$] exhibited a significant preference for the novel object. An unpaired two-sample t-test found no difference in discrimination index between treatment groups [$t(13) = 0.5959$, $p = 0.525$], suggesting that the ketogenic diet did not further enhance object recognition memory. Individual track plots and heat maps for the novel object recognition test are shown in Supplemental Figure 4.

Object placement test (OPT). The object placement test was performed to assess spatial memory. There was no effect of diet on total time spent exploring both objects (data not shown). Performance was quantified by the discrimination index (Figure 4(b)). One sample t-tests found that neither chow-fed mice [$t(6) = 0.9500$, $p = 0.379$] nor keto-fed mice [$t(7) = 1.049$, $p = 0.329$] exhibited a significant preference for the displaced object. An unpaired two-sample t-test found no difference in discrimination index between treatment groups [$t(13) = 0.0907$, $p = 0.465$], suggesting that the ketogenic diet did not yield any measurable benefits in spatial memory on this task. Individual track plots and

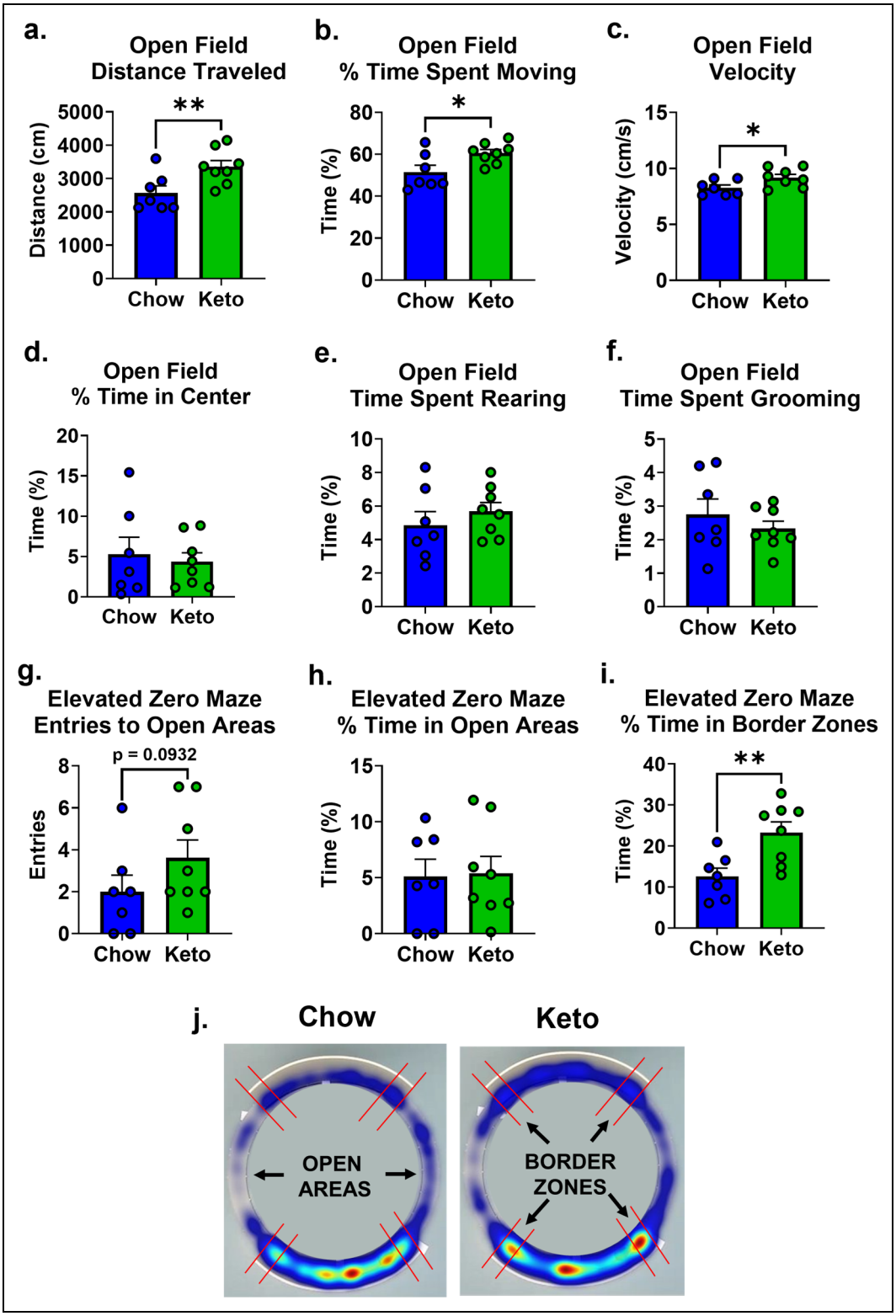

Figure 3. Ketogenic diet increased locomotor/exploratory activity without significantly affecting anxiety-like behavior in male Tg-SwDI mice. Ten-min open field tests were conducted to assess general activity levels and anxiety-related behavior, including measures of (a) distance traveled, (b) time spent moving (%), (c) velocity, (d) center time (%), (e) rearing time (%), and (f) grooming time (%). Five-min elevated zero maze tests were conducted to assess exploratory versus anxiety-like behavior, including measures of (g) number of entries to open areas, (h) time spent in open areas (%), and (i) time spent in border zones (areas within the closed areas that immediately border the open areas). (j) A heatmap of average activity for each group during the elevated zero maze test. Data are presented as mean + SEM in all graphs. All statistical analyses were performed using an unpaired two-sample t-test. *$p < 0.05$, **$p < 0.01$.

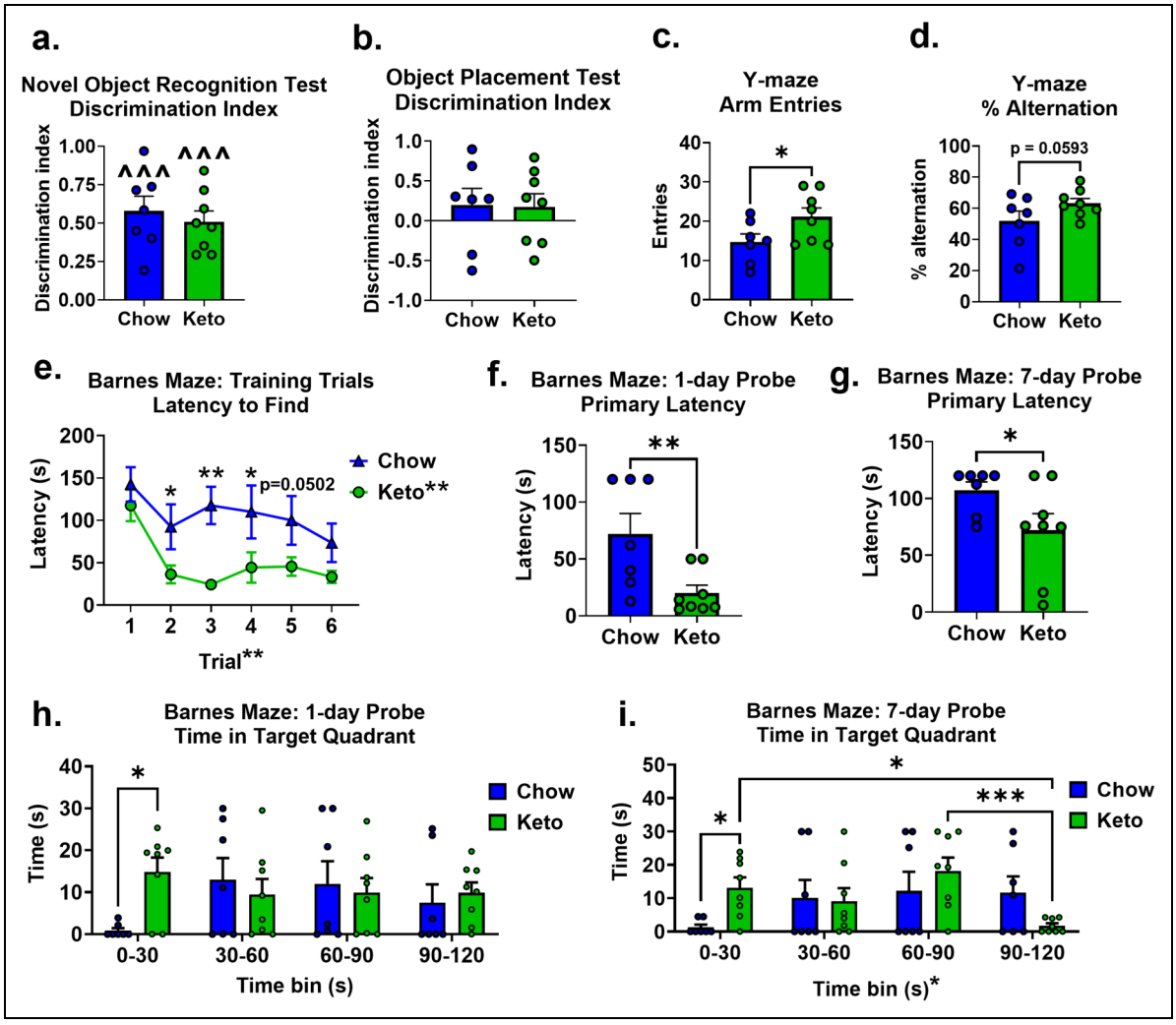

Figure 4. Ketogenic diet improved spatial learning and memory in male Tg-SwDI mice. (a) Novel object recognition test was performed to assess object recognition memory, with training and testing trials separated by 1 h. Time spent with the familiar and novel objects was measured during the 5-min testing trial, and discrimination indices were calculated as a measure of intact memory. (b) Object placement test was performed to assess spatial memory, with training and testing trials separated by 1 h. Time spent with the objects in the familiar and displaced locations was measured during the 5-min testing trial, and discrimination indices were calculated as a measure of intact memory. The Y-maze test was performed to assess spatial working memory, with measures of (c) arm entries and (d) % alternation. The Barnes maze was conducted to assess spatial learning and memory. (e) Latency to find the target hole was measured over six training trials (two trials per day over three days) to assess spatial learning (maximum latency = 180 s). Primary latency, the latency to the first target hole visit, was measured to assess shorter- and longer- term memory during probe trails (f) one and (g) seven days after the last training trials (maximum latency = 120 s). Additionally, for the analysis of probe trials, the Barnes platform was divided into a center zone (30 cm diameter), with the remaining area split into 4 quadrants Time spent in the target quadrant was measured during the (h) 1-day and (i) 7-day probe trials. Data are presented as mean + SEM in all graphs. All statistical analyses were performed using an unpaired two-sample t-test except for Barnes maze training data, which was analyzed using a two-way repeated measures ANOVA followed by Holm-Sidak post hoc test. *$p < 0.05$, **$p < 0.01$, ***$p < 0.001$. ^^^$p < 0.001$ significantly greater than chance performance (hypothetical value of 0).

heat maps for the object placement test are shown in Supplemental Figure 5.

Y-maze. The Y-maze test was performed to assess spatial working memory (Figure 4(c), (d)). Unpaired two-sample t-tests performed separately for each outcome measure revealed that mice fed a ketogenic diet made more arm entries compared to chow-fed mice [$t(13) = 2.086$, $p = 0.029$, Figure 4(c)]. There was also a trend toward enhanced spatial working memory in ketogenic diet-fed mice, as measured by % alternation [$t(13) = 1.671$, $p = 0.059$, Figure 4(d)]. Additional outcome measures, as well as individual track plots and group mean heat maps, for the Y-maze test are shown in Supplemental Figure 6. Briefly, it

was observed that mice fed the ketogenic diet traveled a greater distance in the Y-maze [$t(13) = 2.635$, $p = 0.010$], in line with an increased number of arm entries in this test, and increased distance traveled in the open field. However, there were no group differences in velocity [$t(13) = 0.8538$, $p = 0.204$], suggesting that these differences may be due to differences in exploratory drive rather than motor impairment. Additionally, the trend of improved spontaneous alternation behavior in ketogenic diet fed mice appears to be more due to a reduction in alternate arm returns [$t(13) = 1.476$, $p = 0.082$, trend], rather than same arm returns [$t(13) = 0.1718$, $p = 0.433$]. Importantly, there was no significant preference for entering any particular arm of the Y-maze, with neither group having greater than ~38% preference for any arm (chance = 33%).

Barnes maze. The Barnes maze was performed to assess spatial learning and memory (Figure 4(e)-(i)). Training trials took place over the course of 3 days with two trials per day, and latency to find the escape hole was measured (Figure 4(e)). Across the six training trials, four outliers were identified amongst three different mice in the ketogenic diet group. A two-way repeated measures ANOVA revealed main effects of diet [$F(1,65) = 17.39$, $p = 0.001$; keto < chow] and time [$F(5,65) = 4.116$, $p = 0.003$, decreased latency over trials], with no significant diet×time interaction [$F(5,65) = 0.7321$, $p = 0.602$]. Multiple pairwise comparisons revealed that mice fed a ketogenic diet found the escape hole more quickly than mice fed a standard chow diet on days 25 ($p < 0.05$ for all except day 5, where $p = 0.057$, trend). Individual track plots for Barnes maze training trials are shown in Supplemental Figure 7, while additional outcome measures for the Barnes maze training trials are shown in Supplemental Figure 8. Briefly, separate two-way mixed ANOVAs found a significant main effect of diet for path efficiency [$F(1,13) = 12.30$, $p = 0.004$] and success rate [$F(1,13) = 9.934$, $p = 0.008$], with mice fed a ketogenic diet performing better than mice on standard chow. Multiple pairwise comparisons revealed that mice fed a ketogenic diet had higher path efficiency on trial 4 ($p = 0.023$), with a similar trend on day 5 ($p = 0.087$). Additionally, the number of working memory errors [$F(1,13) = 8.566$, $p = 0.012$], but not reference errors [$F(1,13) = 0.6721$, $p = 0.427$] nor the total number of errors [$F(1,13) = 2.050$, $p = 0.176$], was influenced by diet; mice fed a ketogenic diet made fewer working memory errors overall, with trends of improved performance specifically during trials 3 and 4 ($p < 0.07$ for both).

Barnes maze probe trials were conducted 1 and 7 days after the last training trial to assess spatial memory. Primary latency was defined as the time to the first visit to the target hole location for each probe trial. One outlier was identified in the ketogenic diet group for the 1-day probe. Unpaired two-sample t-tests were performed separately for each probe trial. Mice fed a ketogenic diet were faster to locate the target hole location on both the 1-day probe [$t(13) = 2.869$, $p = 0.007$, Figure 4(f)] and 7-day probe [$t(13) = 2.043$, $p = 0.031$, Figure 4(g)].

Additionally, for each probe trial, the % time spent in the target quadrant, where the escape hole was previously located, was calculated. Each 2-min probe was divided into 30-s time bins to determine exploratory patterns during the trial. For the 1-day probe (Figure 4(h)), a two-way repeated measures ANOVA found that neither the main effect of diet [$F(1,13) = 0.8308$, $p = 0.379$] nor time [$F(3,39) = 0.4136$, $p = 0.744$] were significant; however, there was a trend of a diet×time interaction [$F(3,39) = 2.362$, $p = 0.086$]. Multiple pairwise comparisons found that during the first 30 s of the 1-day probe trial, mice fed a ketogenic diet spent significantly more time in the target quadrant compared to mice fed a standard chow diet ($p = 0.012$). For the 7-day probe (Figure 4(i)), a two-way repeated measures ANOVA found that while the main effect of diet was not significant [$F(1,13) = 0.1633$, $p = 0.693$], there was a significant main effect of time [$F(3,39) = 3.738$, $p = 0.019$] and a diet×time interaction [$F(3,39) = 5.500$, $p = 0.003$]. Multiple pairwise comparisons found that during the first 30 s of the 7-day probe trial, mice fed a ketogenic diet spent significantly more time in the target quadrant compared to mice fed a standard chow diet ($p = 0.036$).

Additional outcome measures and group mean heat maps for the Barnes maze probe trials are shown in Supplemental Figure 8. Briefly, it was observed that mice fed the ketogenic diet traversed the maze with increased velocity during periods of exploration on both 1-day and 7-day probe trials ($p < 0.05$ for both). To determine whether the improved performance during probe trials measured by reduced primary latency could be explained solely due to increased velocity of exploration, we also assessed path efficiency and success rate as outcome measures that are less sensitive to differences in velocity of travel around the maze. It was observed that mice fed the ketogenic diet exhibited trends of increased path efficiency in the 1-day and 7-day probe trials, as well as increased success rate in the 1-day probe trial ($p < 0.09$ for all).

Neuropathological outcomes

Vascular density. Immunohistochemistry was performed to assess vascular density, quantified as the % area covered by Collagen-IV immunolabeling (Figure 5). Measures were taken in the cortex, thalamus, and subregions of the hippocampus (subiculum, dentate gyrus, CA1, and CA3). There was one outlier identified in the cortex and one in the CA3 region in the ketogenic diet group. Unpaired two-sample t-tests were conducted separately for each brain region. While there was an increase in vascular density in the dentate gyrus following chronic administration of

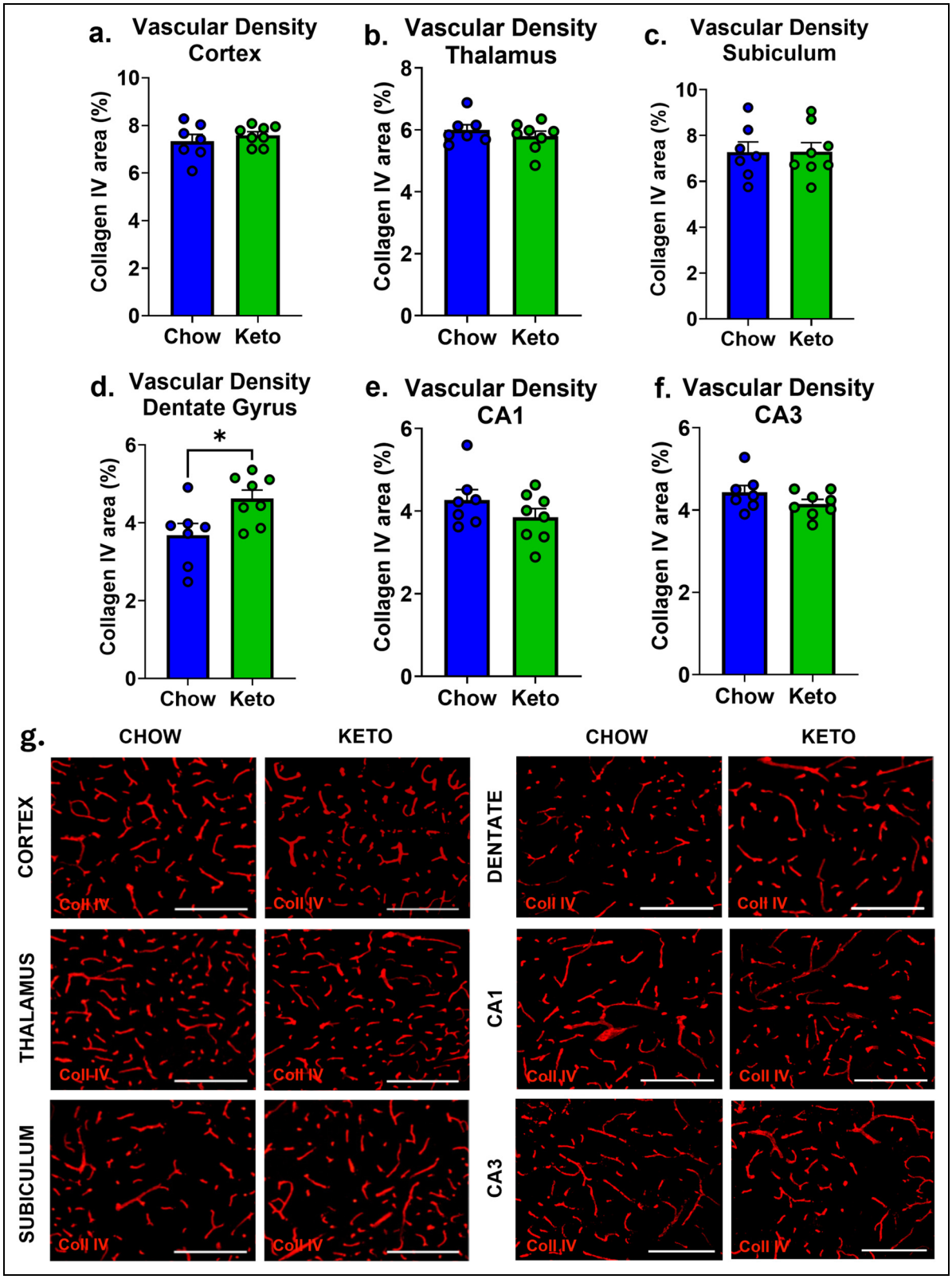

Figure 5. Ketogenic diet increased vascular density in the dentate gyrus in male Tg-SwDI mice. Vascular density was assessed by quantifying the % area covered by Collagen IV immunolabeling in the (a) cortex, (b) thalamus, (c) subiculum, (d) dentate gyrus, (e) CA1, and (f) CA3. (g) Representative images of Collagen IV immunolabeling in each region of interest. Scale bar = 200 μm. Data are presented as mean + SEM in all graphs. All statistical analyses were performed using an unpaired two-sample t-test. *$p < 0.05$.

ketogenic diet [$t(13) = 2.582$, $p = 0.023$, Figure 5(d)], there was no effect of diet on vascular density in the cortex [$t(13) = 0.8198$, $p = 0.427$, Figure 5(a)], thalamus [$t(13) = 0.8565$, $p = 0.407$, Figure 5(b)], subiculum [$t(13) = 0.0333$, $p = 0.974$, Figure 5(c)], CA1 [$t(13) = 1.287$, $p = 0.221$, Figure 5(e)], nor CA3 [$t(13) = 1.447$, $p = 0.172$, Figure 5(f)].

Amyloid pathology. Staining with Thioflavin-S was performed for the localization and quantification of amyloid deposition in the cortex, thalamus, and subregions of the hippocampus (subiculum, dentate gyrus, CA1, and CA3) (Figure 6). Assessment of overall amyloid pathology was measured by the total % area covered by Thioflavin-S staining in each region of interest. There was one outlier identified in the dentate gyrus of the chow-fed group. Unpaired two-sample t-tests were performed separately for each brain region. Ketogenic diet attenuated overall amyloid pathology in the cortex [$t(13) = 2.090$, $p = 0.028$, Figure 6(a)] and dentate gyrus [$t(13) = 4.189$, $p < 0.001$, Figure 6(d)], while there was a trend of decreased amyloid in the subiculum [$t(13) = 1.494$, $p = 0.080$, Figure 6(c)]. There was no effect of diet on overall amyloid pathology in the thalamus [$t(13) = 1.120$, $p = 0.142$, Figure 6(b)], CA1 [$t(13) = 0.5774$, $p = 0.287$, Figure 6(e)], or CA3 [$t(13) = 1.171$, $p = 0.131$, Figure 6(f)].

While amyloid in the dentate gyrus and cortex was clearly deposited as plaque, additional measures were taken to determine the distribution of amyloid in the cerebral vasculature (CAA) and parenchyma in regions with potentially mixed pathology (thalamus, subiculum, CA1, CA3). Cerebral amyloid angiopathy was assessed by the % area of blood vessels covered by amyloid in a given brain region, as calculated by [(area of colocalized Thioflavin-S and Collagen IV)/(area of Collagen IV)] x100. Measures were taken in the thalamus and subregions of the hippocampus (subiculum, CA1, and CA3). One CA1 and one CA3 outlier was identified in the chow-fed group. Unpaired two-sample t-tests were performed separately for each brain region. There was no significant effect of ketogenic diet on CAA in the thalamus [$t(13) = 0.7688$, $p = 0.228$, Figure 6(g)], subiculum [$t(13) = 0.7546$, $p = 0.232$, Figure 6(h)], CA1 [$t(13) = 0.5232$, $p = 0.305$, Figure 6(i)], nor CA3 [$t(13) = 0.0044$, $p = 0.498$, Figure 6(j)].

Parenchymal (non-vascular) amyloid pathology was assessed by measuring the % area covered by Thio-flavin-S staining that was not colocalized with collagen IV immunolabeling (blood vessel marker). Measures were taken in the thalamus and subregions of the hippocampus (subiculum, CA1, and CA3) only, as amyloid pathology in the cortex and dentate were deemed to be plaque/parenchymal, with the overall amyloid measure sufficing for this purpose. One subiculum outlier and one CA1 outlier were identified in the ketogenic diet group. Unpaired two-sample t-tests were performed separately for each brain region. Ketogenic diet attenuated parenchymal (non-vascular) amyloid pathology in the thalamus [$t(13) = 2.188$, $p = 0.024$, Figure 6(k)] and subiculum [$t(13) = 2.781$, $p = 0.008$, Figure 6(l)]. There was no effect of diet on parenchymal amyloid accumulation in the CA1 [$t(13) = 0.7452$, $p = 0.235$, Figure 6(m)] nor CA3 [$t(13) = 1.253$, $p = 0.116$, Figure 6(n)]. Additionally, plaque # was counted in the cortex, with one outlier identified in the ketogenic diet group. An unpaired two-sample t-test found that mice fed a ketogenic diet exhibited an attenuation in plaque # [$t(13) = 2.156$, $p = 0.025$, Figure 6(o)].

Microgliosis. Immunolabeling for ionized calcium-binding adaptor molecule 1 (Iba1) was analyzed as a measure of microgliosis in the cortex, thalamus, and hippocampal subregions (dentate gyrus, subiculum, CA1, CA3; Figure 7). One cortex outlier, one CA1 outlier, and one CA3 outlier were identified in the chow-fed group. Unpaired two-sample t-tests were performed separately for each brain region. There was no effect of diet in the cortex [$t(13) = 0.2818$, $p = 0.783$, Figure 7(a)], thalamus [$t(13) = 1.434$, $p = 0.175$, Figure 7(b)], subiculum [$t(13) = 0.5298$, $p = 0.605$, Figure 7(c)], dentate gyrus [$t(13) = 0.3094$, $p = 0.762$, Figure 7(d)], CA1 [$t(13) = 1.083$, $p = 0.345$, Figure 7(e)], nor CA3 [$t(13) = 1.407$, $p = 0.183$, Figure 7(f)].

Astrogliosis. Immunolabeling for glial fibrillary acidic protein (GFAP) was analyzed as a measure of astrogliosis in the cortex, thalamus, and hippocampal subregions (dentate gyrus, subiculum, CA1, CA3). One mouse in the chow-fed group was identified as having outlier values in both the thalamus and subiculum. Unpaired two-sample t-tests were performed separately for each brain region. In response to a ketogenic diet, there were trends of decreased GFAP immunolabeling in the cortex [$t(13) = 1.789$, $p = 0.097$, Figure 8(a)] and increased GFAP immunolabeling in the thalamus [$t(13) = 2.039$, $p = 0.062$, Figure 8(b)], with no effect of diet in the subiculum [$t(13) = 1.562$, $p = 0.156$, Figure 8(c)], dentate gyrus [$t(13) = 0.5668$, $p = 0.581$, Figure 8(d)], CA1 [$t(13) = 1.347$, $p = 0.201$, Figure 8(e)], nor CA3 [$t(13) = 0.4231$, $p = 0.679$, Figure 8(f)].

Hippocampal neurogenesis. Immunolabeling for Ki67 was used to identify and quantify proliferating cells in the dentate gyrus region of the hippocampus as a measure of cell division during the initial phase of neurogenesis. An unpaired two-sample t-test revealed a trend toward a greater number of Ki67 + cells in mice fed a ketogenic diet compared to chow-fed mice [$t(12) = 1.032$, $p = 0.063$] (Figure 9(a)).

Immunolabeling for doublecortin (DCX) was used to identify and quantify immature neurons/neuroblasts in the dentate gyrus region of the hippocampus as a measure of neurogenesis. An unpaired two-sample t-test found that mice fed a ketogenic diet had a greater number of DCX +

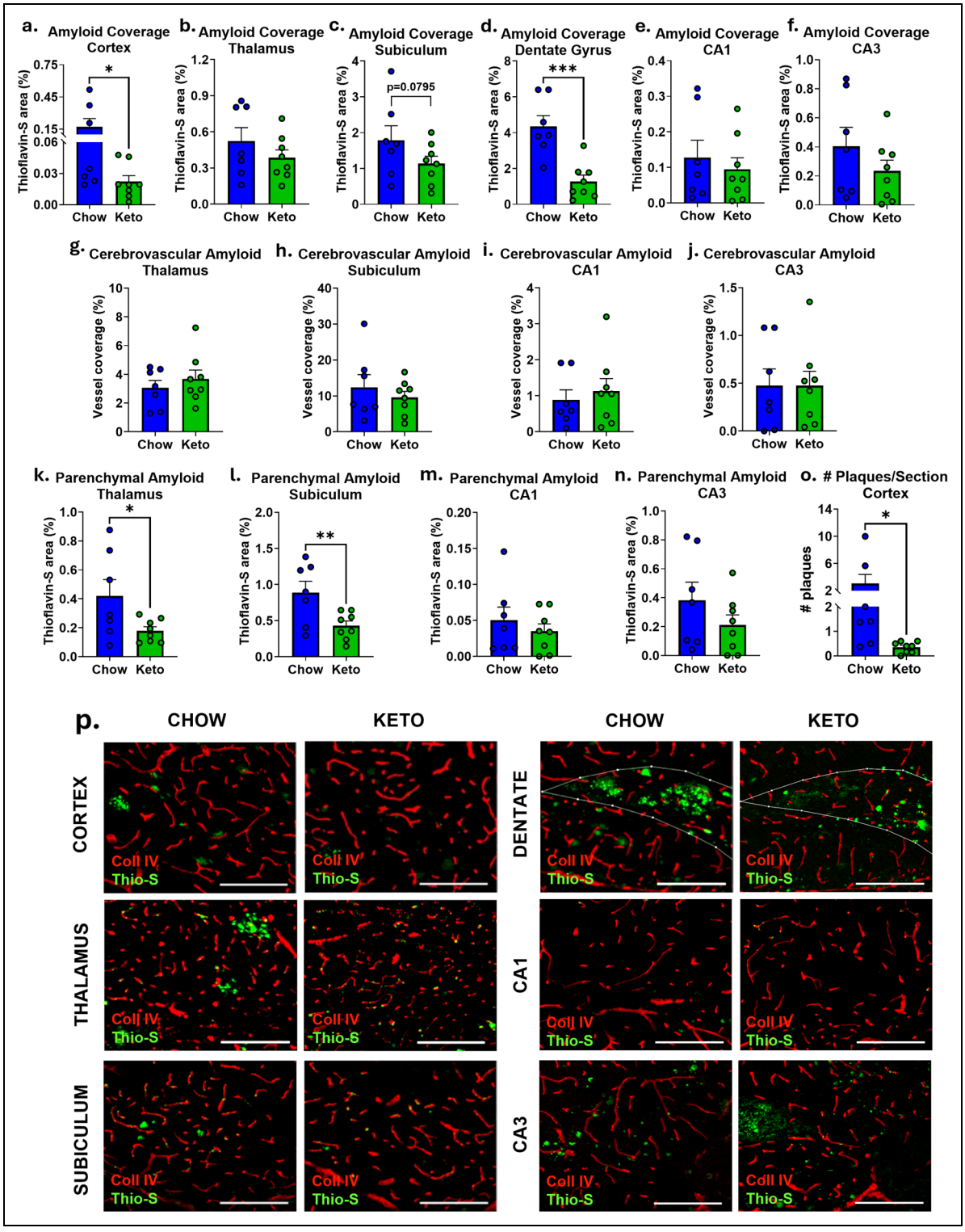

Figure 6. Ketogenic diet attenuated parenchymal amyloid pathology in male Tg-SwDI mice. Thioflavin-S staining was performed to localize and quantify amyloid in the cortex, thalamus, and subregions of the hippocampus. (a-f) Overall amyloid pathology was quantified by measuring the % area covered by thioflavin-S staining in each region of interest. (g-j) Cerebrovascular amyloid, noted in the (g) thalamus, (h) subiculum, (i) CA1, and (j) CA3, was quantified by measuring the percentage of blood vessel area covered by amyloid. (k-n) Parenchymal amyloid deposition was quantified in brain regions exhibiting mixed plaque and CAA pathology. (o) Well-defined, thioflavin-S positive plaques were counted in the cortex. (p) Representative images of Collagen IV immunolabeling (red) and Thioflavin-S staining (green) in each region of interest. Scale bar = 200 μm. Data are presented as mean + SEM in all graphs. All statistical analyses were performed using an unpaired two-sample t-test. *$p < 0.05$, **$p < 0.01$, ***$p < 0.001$.

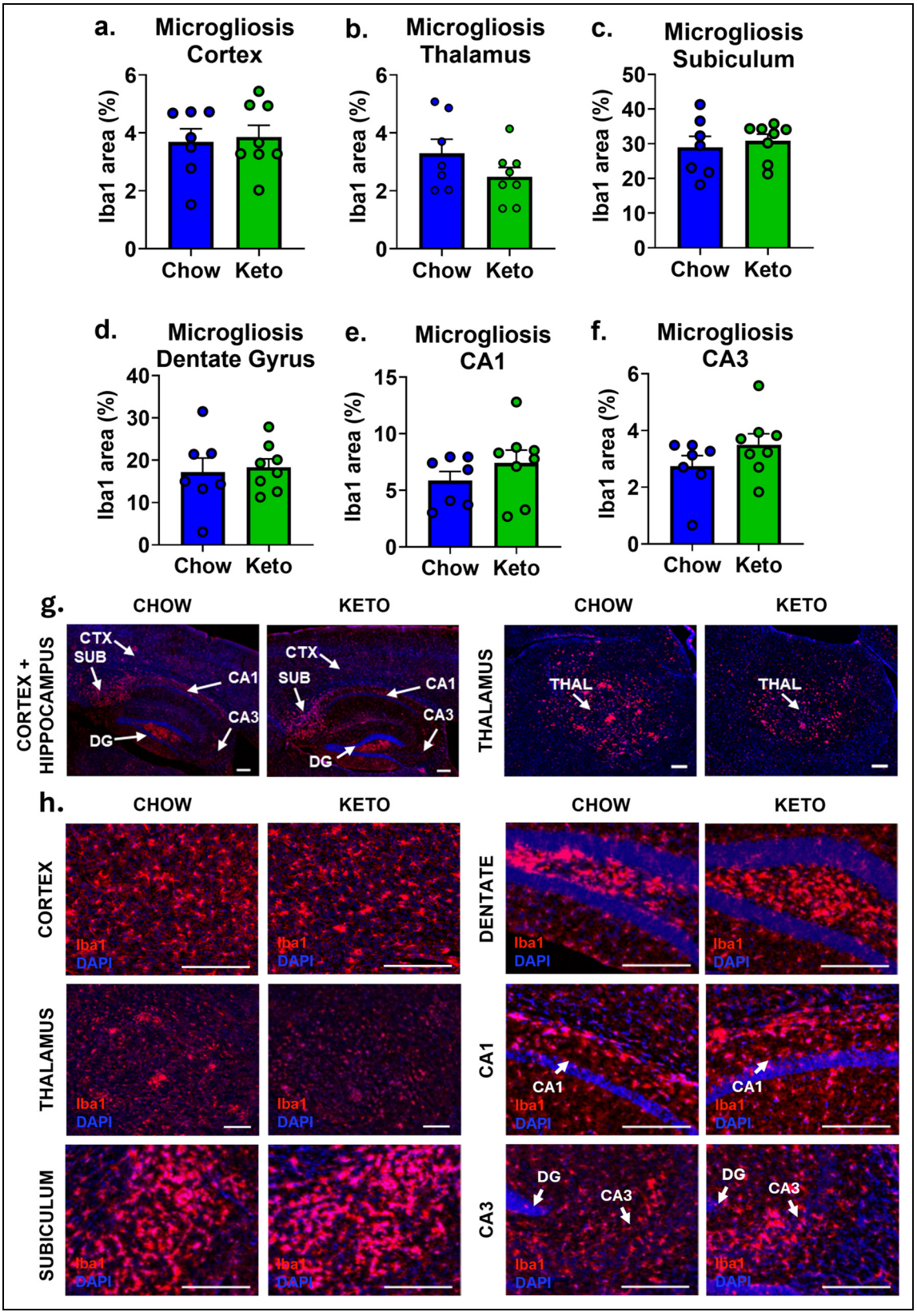

Figure 7. Ketogenic diet did not affect microgliosis in male Tg-SwDI mice. Microgliosis was assessed by quantifying the % area covered by ionized calcium binding adaptor molecule 1 (Iba1) immunolabeling in the (a) cortex, (b) thalamus, (c) subiculum, (d) dentate gyrus, (e) CA1, and (f) CA3. (g) Representative images of Iba1 immunolabeling in each region of interest. Scale bar = 200 μm. Data are presented as mean + SEM in all graphs. All statistical analyses were performed using an unpaired two-sample t-test.

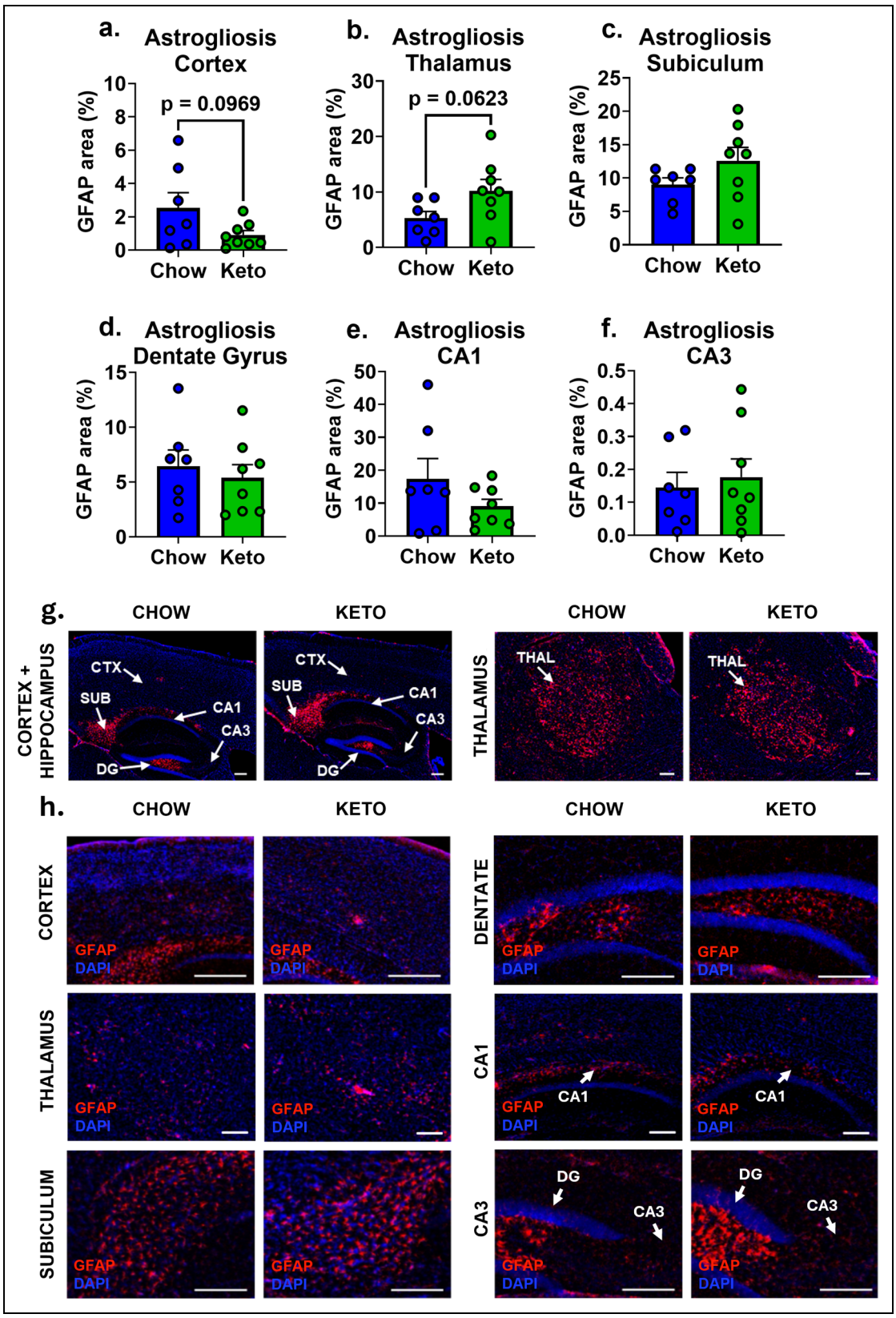

Figure 8. Ketogenic diet had negligible impact on astrogliosis in male Tg-SwDI mice. Astrogliosis was assessed by quantifying the % area covered by glial fibrillary acidic protein (GFAP) immunolabeling in the (a) cortex, (b) thalamus, (c) subiculum, (d) dentate gyrus, (e) CA1, and (f) CA3. (g) Representative images of GFAP immunolabeling in each region of interest. Scale bar = 200 μm. Data are presented as mean + SEM in all graphs. All statistical analyses were performed using an unpaired two-sample t-test.

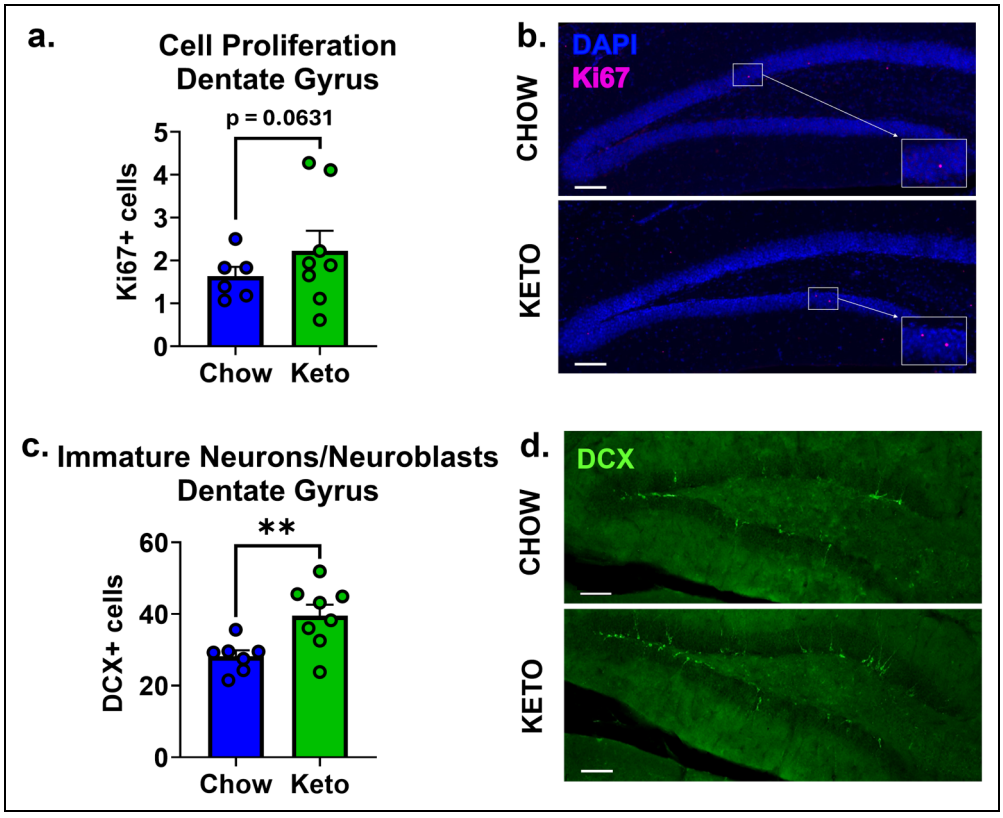

Figure 9. Ketogenic diet enhanced adult hippocampal neurogenesis in male Tg-SwDI mice. (a) Cell proliferation was assessed by counting the number of Ki67 + cells in the dentate gyrus of the hippocampus, as Ki67 immunolabeling is indicative of actively dividing cells during the initial phase of neurogenesis. (b) Representative images of Ki67 immunolabeling in the dentate gyrus. (c) Neurogenesis was assessed by counting the number of doublecortin (DCX)+ cells in the dentate gyrus of the hippocampus, as DCX-immunolabeling is indicative of immature neurons/neuroblasts. (d) Representative images of DCX immunolabeling in the dentate gyrus. Scale bar = 100 µm. Data are presented as mean + SEM in all graphs. All statistical analyses were performed using an unpaired two-sample t-test. *$p < 0.01$.

cells compared to chow-fed mice [$t(13) = 3.073$, $p = 0.005$], indicating an enhancement of neurogenesis (Figure 9(c)).

White matter. Immunolabeling for myelin basic protein (MBP) was used to characterize white matter integrity in the corpus callosum, cortex, and hippocampal subregions [dentate gyrus and stratum lacunosum-moleculare (SLM) layer]. There were no effects of diet on MBP intensity in any area measured, including the corpus callosum [$t(13) = 0.4245$, $p = 0.678$, Figure 10(a)], cortex [$t(13) = 1.486$, $p = 0.161$, Figure 10(b)], dentate gyrus of the hippocampus [$t(13) = 1.263$, $p = 0.229$, Figure 10(c)], nor stratum lacunosum-moleculare (SLM) layer of the hippocampus [$t(13) = 0.5885$, $p = 0.566$, Figure 10(d)].

Discussion

Ketogenic dietary interventions have gained considerable attention in recent years for their potential to combat neurodegenerative diseases, including AD, as well as aid in the recovery from cerebrovascular events, such as stroke.[17,20,22,23,31] However, its utility for the prevention and/or treatment of dementia linked to CAA, a common form of cerebral small vessel disease that increases both the risk of dementia and stroke, has yet to be tested. Here, we fed male Tg-SwDI mice (a transgenic model that exhibits CAA pathology) either standard chow or a ketogenic diet during early- to moderate- stage disease (~3.5–7.5 months of age) and subsequently assessed metabolic, cognitive-behavioral, and neuropathological outcomes. We found that the ketogenic diet resulted in nutritional ketosis, improved several aspects of metabolic and cognitive-behavioral function, attenuated amyloid pathology, and enhanced adult hippocampal neurogenesis. These findings suggest that adherence to a ketogenic diet may provide a safe and effective means of combating dementia in patients with CAA.

The ketogenic diet is characterized by very low carbohydrate intake, moderate protein consumption, and high fat content, resulting in a metabolic state known as "nutritional ketosis". In the absence of sufficient carbohydrate intake, ketone bodies replace glucose as the primary energy

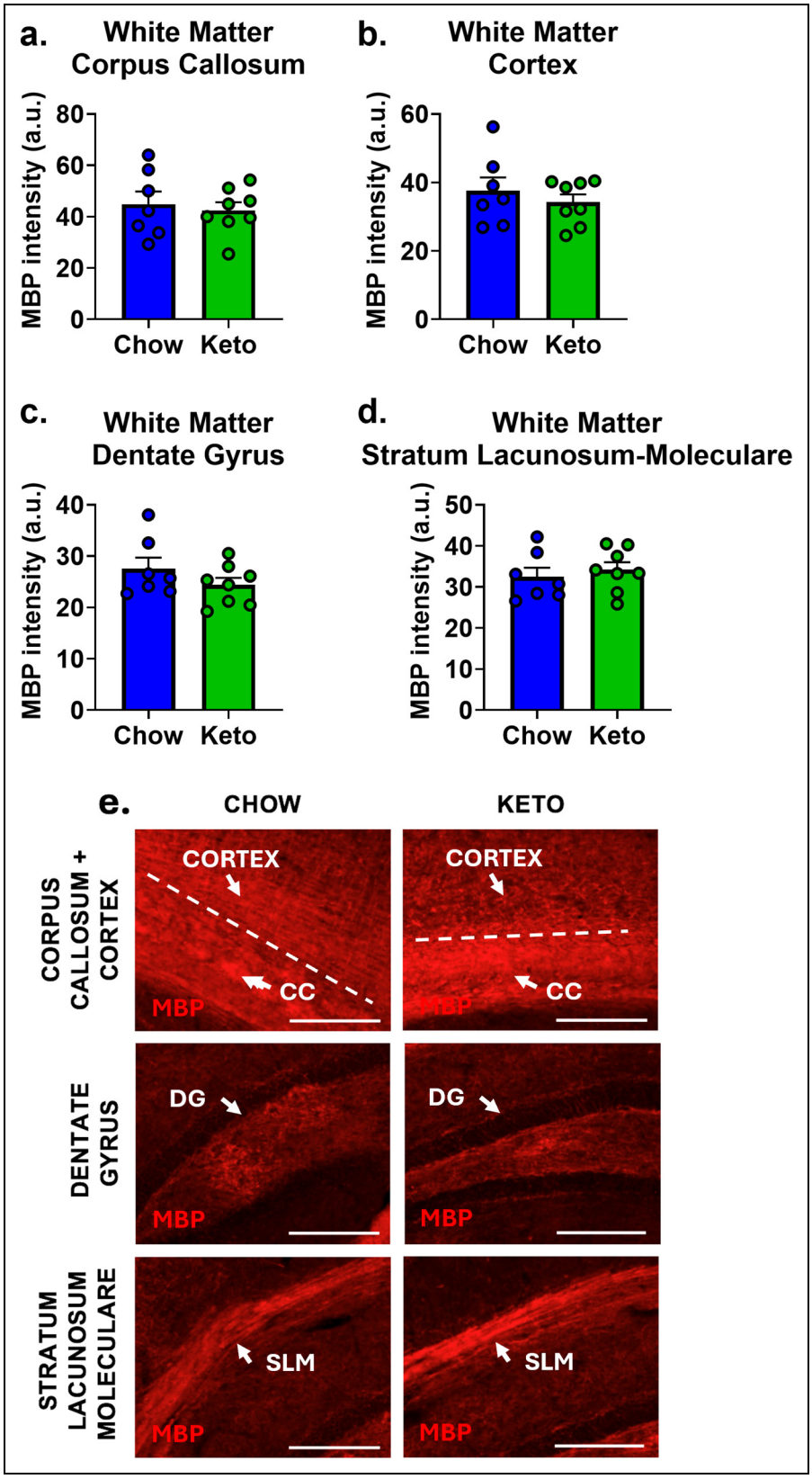

Figure 10. Ketogenic diet did not affect white matter integrity in male Tg-SwDI mice. White matter was assessed by measuring the intensity of MBP immunolabeling in the (a) corpus callosum (CC), (b) cortex, (c) dentate gyrus (DG), and (d) stratum lacunosum-moleculare (SLM). (e) Representative images of myelin basic protein (MBP) immunolabeling in each region of interest. Scale bar = 200 μm. Data are presented as mean + SEM in all graphs. All statistical analyses were performed using an unpaired two-sample t-test.

source. Nutritional ketosis is typically defined by blood ketone levels >0.5 mmol/L. In the present study, our ketogenic diet, with ~3% carbohydrate content, successfully induced nutritional ketosis, with blood ketone levels exceeding this threshold and surpassing those observed in mice fed standard chow.

Despite its high fat content, the ketogenic diet has demonstrated numerous metabolic benefits, including weight loss, management of Type 2 diabetes and dyslipidemia, and attenuation of steatohepatitis.[14,15,32] Consistent with these findings, we report that mice fed a ketogenic diet lost weight compared to baseline, while mice fed a standard chow diet gained weight. Adherence to the ketogenic diet also attenuated fasting and fed blood glucose levels while improving glucose tolerance. Furthermore, visceral fat was reduced, while subcutaneous fat was maintained by a ketogenic diet. Visceral fat, which accumulates around internal organs, is generally considered more harmful than subcutaneous fat, which is located beneath the skin. This difference in fat distribution is associated with varying inflammatory responses and metabolic consequences, with visceral fat generally being more harmful and linked to an increased risk of cardiometabolic and neurodegenerative diseases.[33,34] Studies have shown that individuals with more visceral fat tend to have a higher risk of cognitive decline, reduced white matter integrity, and brain atrophy, particularly in regions critical for memory and cognition, such as the hippocampus.[35,36] Visceral fat is metabolically active, secreting pro-inflammatory cytokines that increase systemic and neuro-inflammation, impair the blood-brain barrier, damage white matter, and contribute to insulin resistance, all of which are linked to cognitive decline and dementia.[36–38] Visceral adiposity is also strongly associated with cardiovascular issues like atherosclerosis, which can diminish cerebral blood flow and increase the risk of dementia.[39,40] In aging and dementia, weight loss and frailty are significant clinical concerns because they exacerbate both physical and cognitive decline.[41,42] Although the ketogenic diet led to mild early weight loss (<10%), body weight began to rebound as the intervention continued. Moreover, subcutaneous fat levels were maintained and activity levels increased in ketogenic diet-fed mice, suggesting that the ketogenic diet may help mitigate frailty and preserve physical function.

Beyond its metabolic benefits, accumulating evidence highlights the ketogenic diet's neuroprotective properties in mitigating neurodegenerative diseases and cerebrovascular events.[43–46] Consistent with preclinical studies demonstrating the cognitive-preserving effects of ketogenic dietary interventions in mouse models of AD and cerebrovascular conditions,[23,47–49] we found that mice fed a ketogenic diet exhibited significant improvements across several cognitive-behavioral domains. Specifically, mice fed a ketogenic diet showed increased exploratory behavior (e.g., open field activity and Y-maze arm entries), aligning with prior findings on the benefits of ketogenic supplements in other AD mouse models.[50] Notably, we have previously shown that exploratory behavior is reduced in Tg-SwDI mice compared to wild-type controls,[28,29] suggesting that the increase observed here likely reflects a restoration of healthy behavior rather than pathological hyperactivity. Anxiety-like behavior, assessed via the open field and elevated zero maze tests, was minimally affected by the ketogenic diet, with subtle increases in open-area exploration likely attributable to enhanced activity levels. In contrast, some previous studies have reported that ketogenic dietary interventions are anxiolytic in other AD mouse models.[50,51] In the current study, the ketogenic diet improved spatial working memory (Y-maze spontaneous alternation), spatial learning, and short- and long-term spatial memory (Barnes maze). Performance on object-based tasks (novel object recognition and object placement tests) did not improve, likely due to task limitations (e.g., ceiling effects for novel object recognition and excessive task difficulty for object placement). Previous studies have similarly reported enhancements in memory and learning tasks with ketogenic dietary interventions in rodent models of AD.[45,47,48]

These improvements in cognitive-behavioral function may be explained, at least in part, by the observed effects of the ketogenic diet on neuropathology and neuroplasticity. We found that the ketogenic diet reduced amyloid pathology, particularly plaque/parenchymal amyloid pathology in the cortex, thalamus, and sub-regions of the hippocampus, including the subiculum and dentate gyrus. This finding aligns with previous work in rodent models demonstrating that ketogenic interventions reduce amyloid burden, potentially contributing to cognitive-behavioral improvements by alleviating synaptic dysfunction and neuronal stress.[48,51,52] There are several mechanisms by which a ketogenic diet could attenuate amyloid pathology,[53] with neuroimmune pathways being one possibility,[54] although we did not observe significant changes in microglial or astrocytic immunolabeling. This diet also improves neuronal energy metabolism by providing ketone bodies as an alternative fuel, boosting mitochondrial function and reducing oxidative stress.[45,53,55] The ketogenic diet may shift amyloid-β protein precursor processing toward a non-amyloidogenic pathway, which could contribute to an overall attenuation of Aβ production. Additionally, improved insulin sensitivity and restored glucose metabolism previously demonstrated to result from ketogenic interventions may further enhance Aβ clearance via proteases like insulin-degrading enzyme.[56] Of note, while non-vascular cerebral amyloid was reduced by the ketogenic diet, the level of vascular amyloid remained unchanged.

Although the ketogenic diet was initiated relatively early in the course of disease, vascular amyloid deposition may be less dynamic or reversible compared to parenchymal amyloid. Previously, we found that while exercise intervention from ~4–12 months of age exerted cognitive-

behavioral benefits and attenuated neuroinflammation, CAA levels were not reduced in mixed-sex Tg-SwDI mice.[28] The persistence of vascular amyloid may be due to the distinct pathways and mechanisms involved in its deposition and clearance being less responsive to the ketogenic diet compared to mechanisms affecting parenchymal amyloid. Vascular amyloid, composed primarily of $A\beta_{40}$, may accumulate earlier than parenchymal amyloid (predominantly $A\beta_{42}$) and may be less responsive to metabolic shifts induced by the diet, though a previous study in an AD mouse model found both $A\beta_{40}$ and $A\beta_{42}$ to be reduced.[52] Once vascular amyloid forms, even at early stages, it may act as a stable seed for further deposition, making it resistant to interventions.[57] Early vascular dysfunction induced by CAA, including damage to smooth muscle and endothelial cells critical for Aβ clearance, may reduce the diet's impact on vascular amyloid. Impaired perivascular drainage, a hallmark of CAA, limits the clearance of vascular amyloid, while enhanced glymphatic system activity demonstrated to result from ketogenic dietary interventions primarily affect parenchymal deposits.[5,58] Future studies should explore the contribution of these potential mechanisms and determine whether combining ketogenic interventions with therapies that target vascular-specific mechanisms, such as enhancing perivascular drainage or restoring endothelial and smooth muscle cell function, may produce additive or synergistic benefits.

Mice fed the ketogenic diet showed increased adult hippocampal neurogenesis, evidenced by an increased number of immature neurons/neuroblasts in the dentate gyrus. Enhanced neurogenesis likely contributes to the observed improvements in spatial learning and memory, as it has been established that hippocampal neurogenesis is critical for cognitive function in this domain.[59,60] Although studies in healthy rodents have generally reported no effect of ketogenic diet on neurogenesis,[61,62] these studies primarily assessed proliferating cells (e.g., Ki67 or BrdU), whereas our findings reflect an increase in immature neurons/neuroblasts (DCX). Analysis of Ki67 + cells revealed only a trend toward increased proliferation in ketogenic diet-fed mice, suggesting that the ketogenic diet may be acting more significantly at later stages of neurogenesis, as reflected by the increase in DCX + cells. Specifically, the ketogenic diet may preferentially promote differentiation into neuronal lineages rather than astrocytic fates and/or enhance the survival and integration of newly generated neurons into hippocampal circuits. While Ki67 and DCX indicate a diet-induced boost in the neurogenic niche, future studies utilizing additional markers (e.g., Sox2/Ascl1/BrdU) will be required to determine the specific progenitor stages affected and the long-term survival of these cells.

Other studies have demonstrated that the ketogenic diet enhances neurogenesis in rodent models of neurological disease, suggesting that the diet may promote neurogenesis specifically in the context of injury, stress, or dysfunction, thereby underscoring its potential to restore neuroplasticity. A ketogenic diet may increase neuroblasts and immature neurons in the dentate gyrus by creating a neuroprotective environment through multiple mechanisms. These include enhanced energy metabolism via ketone bodies, improved mitochondrial function, reduced oxidative stress and inflammation, modulation of epigenetic pathway, such as histone deacetylase inhibition, and upregulation of brain-derived neurotrophic factor, which supports neurogenesis and synaptic plasticity.[63–65]

Interestingly, the ketogenic diet did not appear to confer measurable benefits for neuroinflammation, as indicated by immunofluorescence of astrocytes and microglia, nor for white matter integrity, as assessed by immunofluorescence of myelin basic protein. This contrasts with some studies that have reported reductions in neuroinflammation and improvements in white matter integrity following ketogenic interventions in other models of disease or injury.[23,31,46,47,66,67] This may be due to variations in experimental models, disease stage, and/or dietary formulations.

This study has several limitations that should be addressed in future research. First, we employed a transgenic mouse model of CAA that predominantly models hereditary disease, whereas most human CAA cases are sporadic. This mouse model does not fully replicate all aspects of the human condition. Notably, mice used in this study were young and lacked the age-related arteriosclerosis, hypertension, or endothelial senescence typical of elderly human CAA patients. Introducing a very high fat ketogenic diet to mice with young cerebral vessels may be different from its introduction to aged, calcified, fragile human vessels. Furthermore, there are species differences in lipid metabolism that make mice naturally resistant to atherosclerosis; mice transport cholesterol primarily on HDL, while humans transport cholesterol on LDL. Consequently, a high-saturated-fat diet that is benign in a mouse may be atherogenic in a human, particularly an *APOE4* carrier. Thus, the vascular safety profile of a ketogenic diet in rodents cannot be extrapolated to humans without significant caveats. Future studies should incorporate additional animal models and, ultimately, clinical trials to validate the generalizability of our findings.

Second, our study included only male mice, leaving the influence of biological sex unexplored. There are reported sex differences in cognitive-behavioral performance and neuropathology in Tg-SwDI mice, with females being more adversely affected by the disease.[68–70] We have previously shown striking sex-dependent responses to dietary interventions in other dementia mouse models.[71–73] Given that age and sex significantly influence responses to ketogenic diets in both healthy and diseased states,[47,74–76] follow-up studies should investigate the diet's effects in both sexes to ensure broader applicability.

Third, the ketogenic diet was initiated during early-stage disease. Whether similar benefits would occur at later stages

remains unknown, especially as a recent study reported that ketogenic interventions were effective in earlier but not later-stage disease in 5xFAD mice.[47] Additionally, as the intervention period used in this study was short (4 months), this may be capturing the acute metabolic benefit of ketones without capturing the chronic vascular toxicity of the lipid load associated with a ketogenic diet. The cumulative effects of arterial stiffness, lipid deposition, and glymphatic impairment that could result from chronic consumption of a ketogenic diet may take years to manifest clinically.

Finally, since adherence to a restrictive ketogenic diet is often challenging for elderly patients or those with dementia, future research should explore exogenous ketone supplementation, such as β-hydroxybutyrate. Preliminary evidence suggests that exogenous ketones can improve metabolic and cognitive outcomes in aging and AD, as well as reduce neuroinflammation, mitochondrial dysfunction, and reactive oxygen species, and support neuroplasticity.[18–21] Exogenous ketone supplementation could provide the therapeutic benefits of ketosis while avoiding the potential adverse effects of a diet very high in fat. Therefore, while these results are promising, further research is necessary to confirm these benefits in humans and establish optimal dosing regimens.

Conclusion

In conclusion, our findings demonstrate that a ketogenic diet can induce nutritional ketosis, improve metabolic and cognitive-behavioral functions, reduce amyloid pathology, and enhance neurogenesis in a transgenic mouse model of CAA. These results suggest that ketogenic dietary interventions hold promise as a non-pharmacological strategy for mitigating dementia in those affected by CAA. However, the limitations of this study underscore the need for additional research to refine, validate, and ultimately translate these findings into clinical practice. By addressing these gaps, future studies can further elucidate the therapeutic potential of ketogenic diets and related interventions for neurodegenerative and cerebrovascular diseases.

Acknowledgements

The authors would like to thank Lauren White and Gabriella Albensi for their assistance with fluorescence imaging.

ORCID iDs

Victoria E. Pulido-Correa https://orcid.org/0009-0002-3342-0418
Eleanor J. Wind https://orcid.org/0009-0003-5724-1956
Lisa S. Robison https://orcid.org/0000-0002-5110-9183

Ethical considerations

Not applicable.

Consent to participate

Not applicable.

Author contribution(s)

Victoria E. Pulido-Correa: Conceptualization; Data curation; Formal analysis; Investigation; Methodology; Project administration; Visualization; Writing – original draft; Writing – review & editing.
Ariana V. Hernandez: Investigation; Visualization; Writing – review & editing.
Eleanor J. Wind: Investigation; Methodology; Writing – review & editing.
Yingying Zhu: Investigation; Writing – review & editing.
Chana Vogel: Investigation; Writing – review & editing.
Shaina Binu: Investigation; Writing – review & editing.
Mikayla Jeneske: Investigation; Writing – review & editing.
Dylan Kuni: Investigation; Writing – review & editing.
Vedika Chiduruppa: Investigation; Writing – review & editing.
Bianca Echeverria: Investigation; Writing – review & editing.
Lauren Rosenberg: Investigation; Writing – review & editing.
Lisa S. Robison: Conceptualization; Data curation; Formal analysis; Funding acquisition; Investigation; Methodology; Project administration; Visualization; Writing – original draft; Writing – review & editing.

Funding

The authors disclosed receipt of the following financial support for the research, authorship, and/or publication of this article: This work was supported by the National Institute on Aging [grant number R03 AG081865]; National Institute of Neurological Disorders and Stroke [grant number R16 NS134540]; the American Heart Association [grant number # 946666]; and Nova Southeastern University's College of Psychology.

Declaration of conflicting interests

The authors declared no potential conflicts of interest with respect to the research, authorship, and/or publication of this article.

Data availability statement

The data that support the findings of this study are openly available in Harvard Dataverse at: https://dataverse.harvard.edu/dataverse/Robison_Keto_in_CAA.

Supplemental material

Supplemental material for this article is available online.

References

1. Arvanitakis Z, Leurgans SE, Wang Z, et al. Cerebral amyloid angiopathy pathology and cognitive domains in older persons. *Ann Neurol* 2011; 69: 320–327.
2. Yamada M. Cerebral amyloid angiopathy: emerging concepts. *J Stroke* 2015; 17: 17–30.

3. Alakbarzade V, French JM, Howlett DR, et al. Cerebral amyloid angiopathy distribution in older people: a cautionary note. *Alzheimers Dement (N Y)* 2021; 7: e12145.
4. Haussmann R, Homeyer P, Sauer C, et al. Comorbid cerebral amyloid angiopathy in dementia and prodromal stages-Prevalence and effects on cognition. *Int J Geriatr Psychiatry* 2023; 38: e6015.
5. Kim SH, Ahn JH, Yang H, et al. Cerebral amyloid angiopathy aggravates perivascular clearance impairment in an Alzheimer's disease mouse model. *Acta Neuropathol Commun* 2020; 8: 181.
6. Greenberg SM, Bacskai BJ, Hernandez-Guillamon M, et al. Cerebral amyloid angiopathy and Alzheimer disease - one peptide, two pathways. *Nat Rev Neurol* 2020; 16: 30–42.
7. Salloway S, Chalkias S, Barkhof F, et al. Amyloid-related imaging abnormalities in 2 phase 3 studies evaluating aducanumab in patients with early Alzheimer disease. *JAMA Neurol* 2022; 79: 13–21.
8. Honig LS, Barakos J, Dhadda S, et al. ARIA In patients treated with lecanemab (BAN2401) in a phase 2 study in early Alzheimer's disease. *Alzheimers Dement (N Y)* 2023; 9: e12377.
9. Cummings J, Apostolova L, Rabinovici GD, et al. Lecanemab: appropriate use recommendations. *J Prev Alzheimers Dis* 2023; 10: 362–377.
10. van Dyck CH, Sabbagh M and Cohen S. Lecanemab in early Alzheimer's disease. *Reply. N Engl J Med* 2023; 388: 1631–1632.
11. Greenberg SM, Cordonnier C, Schneider JA, et al. Off-label use of aducanumab for cerebral amyloid angiopathy. *Lancet Neurol* 2021; 20: 596–597.
12. Sin MK, Zamrini E, Ahmed A, et al. Anti-amyloid therapy, AD, and ARIA: untangling the role of CAA. *J Clin Med* 2023; 12: 6792.
13. Masood W, Annamaraju P, Khan Suheb MZ, et al. *Ketogenic diet. StatPearls*. Treasure Island, FL: StatPearls Publishing, 2024.
14. Luo W, Zhang J, Xu D, et al. Low carbohydrate ketogenic diets reduce cardiovascular risk factor levels in obese or overweight patients with T2DM: a meta-analysis of randomized controlled trials. *Front Nutr* 2022; 9: 1092031.
15. Zhou C, Wang M, Liang J, et al. Ketogenic diet benefits to weight loss, glycemic control, and lipid profiles in overweight patients with type 2 diabetes mellitus: a meta-analysis of randomized controlled trails. *Int J Environ Res Public Health* 2022; 19: 10429.
16. Chinna-Meyyappan A, Gomes FA, Koning E, et al. Effects of the ketogenic diet on cognition: a systematic review. *Nutr Neurosci* 2023; 26: 1258–1278.
17. Tao Y, Leng SX and Zhang H. Ketogenic diet: an effective treatment approach for neurodegenerative diseases. *Curr Neuropharmacol* 2022; 20: 2303–2319.
18. Makievskaya CI, Popkov VA, Andrianova NV, et al. Ketogenic diet and ketone bodies against ischemic injury: targets, mechanisms, and therapeutic potential. *Int J Mol Sci* 2023; 24: 2576.
19. Saito ER, Warren CE, Hanegan CM, et al. A novel ketone-supplemented diet improves recognition memory and hippocampal mitochondrial efficiency in healthy adult mice. *Metabolites* 2022; 12: 1019.
20. Shippy DC, Wilhelm C, Viharkumar PA, et al. β-Hydroxybutyrate inhibits inflammasome activation to attenuate Alzheimer's disease pathology. *J Neuroinflammation* 2020; 17: 280.
21. Youm YH, Nguyen KY, Grant RW, et al. The ketone metabolite β-hydroxybutyrate blocks NLRP3 inflammasome-mediated inflammatory disease. *Nat Med* 2015; 21: 263–269.
22. Hersant H and Grossberg G. The ketogenic diet and Alzheimer's disease. *J Nutr Health Aging* 2022; 26: 606–614.
23. Gibson CL, Murphy AN and Murphy SP. Stroke outcome in the ketogenic state–a systematic review of the animal data. *J Neurochem* 2012; 123: 52–57.
24. Percie du Sert N, Hurst V, Ahluwalia A, et al. The ARRIVE guidelines 2.0: updated guidelines for reporting animal research. *PLoS Biol* 2020; 18: e3000410.
25. Davis J, Xu F, Deane R, et al. Early-onset and robust cerebral microvascular accumulation of amyloid beta-protein in transgenic mice expressing low levels of a vasculotropic Dutch/Iowa mutant form of amyloid beta-protein precursor. *J Biol Chem* 2004; 279: 20296–20306.
26. Rosas-Hernandez H, Cuevas E, Raymick JB, et al. Impaired amyloid beta clearance and brain microvascular dysfunction are present in the Tg-SwDI mouse model of Alzheimer's disease. *Neuroscience* 2020; 440: 48–55.
27. Xu F, Grande AM, Robinson JK, et al. Early-onset subicular microvascular amyloid and neuroinflammation correlate with behavioral deficits in vasculotropic mutant amyloid beta-protein precursor transgenic mice. *Neuroscience* 2007; 146: 98–107.
28. Robison LS, Popescu DL, Anderson ME, et al. Long-term voluntary wheel running does not alter vascular amyloid burden but reduces neuroinflammation in the Tg-SwDI mouse model of cerebral amyloid angiopathy. *J Neuroinflammation* 2019; 16: 144.
29. Robison LS, Francis N, Popescu DL, et al. Environmental enrichment: disentangling the influence of novelty, social, and physical activity on cerebral amyloid angiopathy in a transgenic mouse model. *Int J Mol Sci* 2020; 21: 843.
30. Kraeuter AK, Guest PC and Sarnyai Z. The Y-maze for assessment of spatial working and reference memory in mice. *Methods Mol Biol* 2019; 1916: 105–111.
31. Guo M, Wang X, Zhao Y, et al. Ketogenic diet improves brain ischemic tolerance and inhibits NLRP3 inflammasome activation by preventing Drp1-mediated mitochondrial fission and endoplasmic reticulum stress. *Front Mol Neurosci* 2018; 11: 86.
32. Luukkonen PK, Dufour S, Lyu K, et al. Effect of a ketogenic diet on hepatic steatosis and hepatic mitochondrial

metabolism in nonalcoholic fatty liver disease. *Proc Natl Acad Sci U S A* 2020; 117: 7347–7354.
33. Dolatshahi M, Commean PK, Rahmani F, et al. Alzheimer disease pathology and neurodegeneration in midlife obesity: a pilot study. *Aging Dis* 2024; 15: 1843–1854.
34. Huang X, Wang YJ and Xiang Y. Bidirectional communication between brain and visceral white adipose tissue: its potential impact on Alzheimer's disease. *EBioMedicine* 2022; 84: 104263.
35. Ozato N, Saitou S, Yamaguchi T, et al. Association between visceral fat and brain structural changes or cognitive function. *Brain Sci* 2021; 11: 1036.
36. O'Brien PD, Hinder LM, Callaghan BC, et al. Neurological consequences of obesity. *Lancet Neurol* 2017; 16: 465–477.
37. Lampe L, Zhang R, Beyer F, et al. Visceral obesity relates to deep white matter hyperintensities via inflammation. *Ann Neurol* 2019; 85: 194–203.
38. Xu H, Barnes GT, Yang Q, et al. Chronic inflammation in fat plays a crucial role in the development of obesity-related insulin resistance. *J Clin Invest* 2003; 112: 1821–1830.
39. Laurin D, Masaki KH, White LR, et al. Ankle-to-brachial index and dementia: the Honolulu-Asia Aging Study. *Circulation* 2007; 116: 2269–2274.
40. Xie B, Shi X, Xing Y, et al. Association between atherosclerosis and Alzheimer's disease: a systematic review and meta-analysis. *Brain Behav* 2020; 10: e01601.
41. Halil M, Cemal Kizilarslanoglu M, Emin Kuyumcu M, et al. Cognitive aspects of frailty: mechanisms behind the link between frailty and cognitive impairment. *J Nutr Health Aging* 2015; 19: 276–283.
42. Franx BAA, Arnoldussen IAC, Kiliaan AJ, et al. Weight loss in patients with dementia: considering the potential impact of pharmacotherapy. *Drugs Aging* 2017; 34: 425–436.
43. Rong L, Peng Y, Shen Q, et al. Effects of ketogenic diet on cognitive function of patients with Alzheimer's disease: a systematic review and meta-analysis. *J Nutr Health Aging* 2024; 28: 100306.
44. Wu L, Chu L, Pang Y, et al. Effects of dietary supplements, foods, and dietary patterns in Parkinson's disease: meta-analysis and systematic review of randomized and crossover studies. *Eur J Clin Nutr* 2024; 78: 365–375.
45. Oliveira TPD, Morais ALB, Dos Reis PLB, et al. A potential role for the ketogenic diet in Alzheimer's disease treatment: exploring pre-clinical and clinical evidence. *Metabolites* 2023; 14: 25.
46. Jang J, Kim SR, Lee JE, et al. Molecular mechanisms of neuroprotection by ketone bodies and ketogenic diet in cerebral ischemia and neurodegenerative diseases. *Int J Mol Sci* 2023; 25: 124.
47. Xu Y, Jiang C, Wu J, et al. Ketogenic diet ameliorates cognitive impairment and neuroinflammation in a mouse model of Alzheimer's disease. *CNS Neurosci Ther* 2022; 28: 580–592.
48. Qin Y, Bai D, Tang M, et al. Ketogenic diet alleviates brain iron deposition and cognitive dysfunction via Nrf2-mediated ferroptosis pathway in APP/PS1 mouse. *Brain Res* 2023; 1812: 148404.
49. Beckett TL, Studzinski CM, Keller JN, et al. A ketogenic diet improves motor performance but does not affect β-amyloid levels in a mouse model of Alzheimer's disease. *Brain Res* 2013; 1505: 61–67.
50. Pawlosky RJ, Kashiwaya Y, King MT, et al. A dietary ketone ester normalizes abnormal behavior in a mouse model of Alzheimer's disease. *Int J Mol Sci* 2020; 21: 1044.
51. Kashiwaya Y, Bergman C, Lee JH, et al. A ketone ester diet exhibits anxiolytic and cognition-sparing properties, and lessens amyloid and tau pathologies in a mouse model of Alzheimer's disease. *Neurobiol Aging* 2013; 34: 1530–1539.
52. Van der Auwera I, Wera S, Van Leuven F, et al. A ketogenic diet reduces amyloid beta 40 and 42 in a mouse model of Alzheimer's disease. *Nutr Metab (Lond)* 2005; 2: 28.
53. Taylor MK, Sullivan DK, Keller JE, et al. Potential for ketotherapies as amyloid-regulating treatment in individuals at risk for Alzheimer's disease. *Front Neurosci* 2022; 16: 899612.
54. Jorfi M, Maaser-Hecker A and Tanzi RE. The neuroimmune axis of Alzheimer's disease. *Genome Med* 2023; 15: 6.
55. Pinto A, Bonucci A, Maggi E, et al. Anti-oxidant and anti-inflammatory activity of ketogenic diet: new perspectives for neuroprotection in Alzheimer's disease. *Antioxidants (Basel)* 2018; 7: 63.
56. Farris W, Mansourian S, Chang Y, et al. Insulin-degrading enzyme regulates the levels of insulin, amyloid β-protein, and the β-amyloid precursor protein intracellular domain in vivo. *Proc Natl Acad Sci U S A* 2003; 100: 4162–4167.
57. Xu F, Fu Z, Dass S, et al. Cerebral vascular amyloid seeds drive amyloid β-protein fibril assembly with a distinct anti-parallel structure. *Nat Commun* 2016; 7: 13527.
58. Tan X, Li X, Li R, et al. β-hydroxybutyrate alleviates neurological deficits by restoring glymphatic and inflammation after subarachnoid hemorrhage in mice. *Exp Neurol* 2024; 378: 114819.
59. Lieberwirth C, Pan Y, Liu Y, et al. Hippocampal adult neurogenesis: its regulation and potential role in spatial learning and memory. *Brain Res* 2016; 1644: 127–140.
60. Frechou MA, Martin SS, McDermott KD, et al. Adult neurogenesis improves spatial information encoding in the mouse hippocampus. *Nat Commun* 2024; 15: 6410.
61. Strandberg J, Kondziella D, Thorlin T, et al. Ketogenic diet does not disturb neurogenesis in the dentate gyrus in rats. *Neuroreport* 2008; 19: 1235–1237.
62. Irfannuddin I, Sarahdeaz SFP, Murti K, et al. The effect of ketogenic diets on neurogenesis and apoptosis in the dentate gyrus of the male rat hippocampus. *J Physiol Sci* 2021; 71: 3.
63. Pinto A, Bonucci A, Maggi E, et al. Anti-oxidant and anti-inflammatory activity of ketogenic diet: new perspectives for neuroprotection in Alzheimer's disease. *Antioxidants (Basel)* 2018; 7: 63.
64. Kim SW, Marosi K and Mattson M. Ketone beta-hydroxybutyrate up-regulates BDNF expression through NF-κB as an adaptive response against ROS, which may

improve neuronal bioenergetics and enhance neuroprotection (P3.090). *Neurology* 2017; 88: P3.090.
65. Wang X, Wu X, Liu Q, et al. Ketogenic metabolism inhibits histone deacetylase (HDAC) and reduces oxidative stress after spinal cord injury in rats. *Neuroscience* 2017; 366: 36–43.
66. Jiang J, Pan H, Shen F, et al. Ketogenic diet alleviates cognitive dysfunction and neuroinflammation in APP/PS1 mice via the Nrf2/HO-1 and NF-κB signaling pathways. *Neural Regen Res* 2023; 18: 2767–2772.
67. Mu J, Wang T, Li M, et al. Ketogenic diet protects myelin and axons in diffuse axonal injury. *Nutr Neurosci* 2022; 25: 1534–1547.
68. Maniskas ME, Mack AF, Morales-Scheihing D, et al. Sex differences in a murine model of cerebral amyloid angiopathy. *Brain Behav Immun Health* 2021; 14: 100260.
69. Setti SE, Flanigan T, Hanig J, et al. Assessment of sex-related neuropathology and cognitive deficits in the Tg-SwDI mouse model of Alzheimer's disease. *Behav Brain Res* 2022; 428: 113882.
70. Finger C, Lee J and Manwani B. Sex differences in cerebral amyloid angiopathy: the role of monocytes/macrophages (S2.008). *Neurology* 2022; 98: 3443.
71. Robison LS, Gannon OJ, Thomas MA, et al. Role of sex and high-fat diet in metabolic and hypothalamic disturbances in the 3xTg-AD mouse model of Alzheimer's disease. *J Neuroinflammation* 2020; 17: 285.
72. Gannon OJ, Robison LS, Salinero AE, et al. High-fat diet exacerbates cognitive decline in mouse models of Alzheimer's disease and mixed dementia in a sex-dependent manner. *J Neuroinflammation* 2022; 19: 110.
73. Salinero AE, Robison LS, Gannon OJ, et al. Sex-specific effects of high-fat diet on cognitive impairment in a mouse model of VCID. *FASEB J* 2020; 34: 15108–15122.
74. Cochran J, Taufalele PV, Lin KD, et al. Sex differences in the response of C57BL/6 mice to ketogenic diets. *Diabetes* 2018; 67: 1884-P.
75. Eap B, Nomura M, Panda O, et al. Ketone body metabolism declines with age in mice in a sex-dependent manner. *bioRxiv* 2022: 2022.2010.2005.511032 [Preprint]. Posted November 02, 2022.
76. Kumar M, Bhatt B, Gusain C, et al. Sex-specific effects of ketogenic diet on anxiety-like behavior and neuroimmune response in C57Bl/6J mice. *J Nutr Biochem* 2024; 127: 109591.